8-2014

Historical Demography and Dispersal Patterns in the Eastern Pipistrelle Bat (*Perimyotis subflavus*)

Alynn M. Martin
Grand Valley State University

Historical Demography and Dispersal Patterns in the Eastern Pipistrelle Bat (*Perimyotis subflavus*)

Alynn M. Martin

A Thesis Submitted to the Graduate Faculty of

GRAND VALLEY STATE UNIVERSITY

In

Partial Fulfillment of the Requirements

For the Degree of

Master of Science

Biology

August 2014

ACKNOWLEDGEMENTS

I would like to thank my advisor and committee chair, Amy Russell, and the members of my graduate committee, Michael Henshaw and Maarten Vonhof, for their continued support and guidance throughout my Master's program. I would also like to thank Susan Munster, Meg Woller-Skar, Ira Woodring, Laura Kirby, and Jessica Pontow, who offered me their expertise, time, and skills to make this project excel. Lastly, I would like to thank my family for always encouraging me to pursue my academic goals.

ABSTRACT

The recent emergence of threats to North American bat conservation has prompted increased population genetics research on high risk species. The eastern pipistrelle bat is affected by both white-nose syndrome and wind turbine mortality. However, little work has been done regarding the population structure and effective population size of this species. Using the HVI region of the mitochondria and eight microsatellite loci, I analyzed male and female structure across the sample range of *P. subflavus* and estimated the effective population size of their populations. Pairwise F_{ST} values indicate that there is one panmictic population based on microsatellite data, while mitochondrial data supports two populations within the sampled range. AMOVA results suggest that females are making short distance movements (ϕ_{SC} = 9.23%). Mitochondrial and microsatellite data showed contrasting results for effective population size and size change over time. Mitochondrial data suggest an increase in female effective size for both Appalachian and West populations in the past 15,000 to 28,000 years from ~15,000 individuals to 400,000. Microsatellite data further suggest a recent bottleneck from a large ancestral population (1.55 x 10^6), leaving a small current effective population of 9,000 (95% HPDI 10, 3.78 x 10^6) individuals. The persistence of the eastern pipistrelle is dependent upon the maintenance of genetic diversity, and calls for the conservation of genetically distinct populations as well as the preservation of hibernacula and swarming locations.

TABLE OF CONTENTS

List of Tables

List of Figures

INTRODUCTION

Molecular tools have become increasingly useful in understanding the behavior, ecology, and evolution of non-model species (Vignal *et al.* 2002). Molecular genetics has the potential to expose life history information that would otherwise be difficult to observe, but could provide relevant information for conservation efforts. Such information includes the identification of barriers to gene flow, the estimation of rates of migration, the inference of changes in population size, and the reconstruction of colonization events (Luikart *et al.* 1998; Xu *et al.* 2010; Buchalski *et al.* 2014). Molecular methods have proven particularly useful in dealing with organisms that are difficult to study due to their elusive nature or access-limiting habitats, including elephants (Eggert *et al.* 2003), gorillas (Guschanski *et al.* 2009), bears (Bellemain *et al.* 2005), and bats (Burland and Worthington Wilmer 2001; Moussy *et al.* 2013). Bats pose a particular challenge because they are long-lived, nocturnal, and exhibit complex life cycles (Burland and Worthington Wilmer 2001). However, in the past decade population genetic studies have been used to reveal patterns of genetic structure and gene flow (Carstens *et al.* 2004; Russell *et al.* 2005; Chen *et al.* 2006; Vonhof *et al.* 2008; Lu *et al.* 2013) and evidence for (Petit *et al.* 2001; Kerth *et al.* 2002; Rivers *et al.* 2006; Arnold 2007; Nagy *et al.* 2013; Miller-Butterworth *et al.* 2014) or against (Sun *et al.* 2012) sex-biased dispersal in various bat species.

Dispersal is a unidirectional movement by which individuals move away from their natal location (Fleming and Eby 2003). Sex-biased dispersal is the preferential movement of one sex away from the natal site to breed while the other sex remains in or continually returns to the same location (Greenwood 1980; Handley and Perrin 2007). This behavior is commonly observed in both mammals and birds; but dispersal in mammals is often male-biased, while female-biased dispersal predominates in birds (Greenwood 1980). In bat species where the

mating system is polygynous, it is typical for males to disperse while females exhibit philopatry (McCracken and Wilkinson 2000; Kerth *et al.* 2002; Senior *et al.* 2005; Arnold 2007; Safi *et al.* 2007; Chen *et al.* 2008). Potential benefits to female philopatry include familiarity with known roosts during the rearing of young, knowledge of food sources, and kin cooperation, while male dispersal benefits may include maximization of mate access and resource availability (Handley and Perrin 2007).

While restricted gene flow may result in genetic structure and possible inbreeding, bat species exhibiting limited physical dispersal may engage in other behaviors that promote genetic admixture. In temperate species it is typical for males and females to roost together during hibernation in winter months, segregate post-hibernation in the spring and summer when females form maternity colonies and males live alone or in bachelor colonies, and then co-roost again during autumnal swarming (Kerth *et al.* 2003; Rivers *et al.* 2005; Rivers *et al.* 2006; Furmankiewicz and Altringham 2007; Altringham 2011). Because these life stages may take place over a broad geographic area (Fleming and Eby 2003), the timing of migration is a key factor when analyzing gene flow in bat populations. Migration is a bidirectional movement by which bats relocate to a more favorable climate or roost during winter months and return to their original summer location in the spring (Fleming and Eby 2003; Rivers *et al.* 2006; Cryan and Veilleux 2007; Altringham 2011; Krauel and McCracken 2013). Migratory movements are described as habitat shifts of 50 km or greater but can be as extensive as 1700 km (Fleming and Eby 2003; Altringham 2011). There tends to be female-biased migration in temperate bat species where females are more likely to migrate in general and move farther distances than males (Fleming and Eby 2003; Kurta 2010; Krauel and McCracken 2013). Species of bats in which one or both of the sexes exhibit site fidelity but take part in long distance migrations (≥1000 km) are

less likely to have genetic substructure and more likely to have higher effective population sizes than sedentary species (Fleming and Eby 2003; Furmankiewicz and Altringham 2007).

Migratory events allow for contact and potential mating among individuals from different regions. Following migration but preceding hibernation, an opportunity for genetic connectivity occurs through a behavior known as swarming (Kerth *et al.* 2003; Rivers *et al.* 2005; Rivers *et al.* 2006; Furmankiewicz and Altringham 2007). During swarming events, large numbers of bats congregate inside or around hibernacula to engage in activities including information exchange, chasing, and mating (Kerth *et al.* 2003; Parsons *et al.* 2003; Rivers *et al.* 2005; Rivers *et al.* 2006; Furmankiewicz and Altringham 2007). Mating during swarming may be responsible for gene flow among otherwise isolated summer colonies, increasing genetic diversity and effective population size (Furmankiewicz and Altringham 2007).

Population genetic approaches have often been used to make inferences about sex-biased dispersal in bats (Kerth *et al.* 2002; Arnold 2007; Chen *et al.* 2008). In populations where females exhibit seasonal philopatry to maternity roosts, detectable gene flow has been thought to be predominately effected by males and thus dependent upon how far males disperse from their natal sites (Chen *et al.* 2008). Markers with different modes of inheritance, bi-parental and sex-specific, would typically be used to address questions regarding sex-biased dispersal (Prugnolle and de Meeus 2002). Comparisons of nuclear markers with sex-specific markers (typically female-inherited mitochondrial DNA) were commonly used to infer differences in patterns of movement between the sexes (Prugnolle and de Meeus 2002).

Promiscuous mating during fall swarming can complicate inferences of sex-biased dispersal within and among swarming catchment areas (Rivers *et al.* 2005; Rivers *et al.* 2006). In particular, this can lead to false inferences of sex-biased dispersal through the typical approach

of comparing sex-specific markers to nuclear autosomal markers. For example, if mating occurs randomly at regional swarming sites, then no genetic structure within the catchment area would be expected at nuclear loci even if both males and females exhibit summer site fidelity. Under those same conditions, population structure at mitochondrial markers would be expected among maternity colonies but not male roosts within a catchment area. In other words, for species with this swarming behavior, the catchment area becomes the population, and analyses of population structure among summer colonies can be used to define the geographic reach of catchment areas (Figure 1).

North American temperate vespertilionid bats are thought to exhibit male-biased dispersal (*Corynorhinus* spp., Piaggio *et al.* 2009a; *Eptesicus fuscus*, Turmelle *et al.* 2011), consistent with the predominant mammalian pattern. Another North American vespertilionid, the eastern pipistrelle bat (*Perimyotis subflavus*) is commonly assumed to follow the same pattern of male-biased dispersal across its range, yet little work has been done to test that assumption. Radio-tracking studies have indicated that female *P. subflavus* exhibit fidelity to their summer roost location both within and between years (Veilleux and Veilleux 2004; Poissant 2009), and that juvenile females tend to return to their natal site in subsequent years (Veilleux and Veilluex 2004). Additionally, stable isotope analyses suggest that males complete longer north-south migratory movements than females (Fraser *et al.* 2012). Stable isotope and wind turbine mortality data redefined the movement tendencies and capabilities of *P. subflavus*, which had historically been understood as being limited to short distance movements of 100 km or less (Griffin 1940; Barbour and Davis 1969; Fujita and Kunz 1984), and could have direct implications for genetic connectivity in this species. A molecular analysis of *P. subflavus*

populations would provide additional evidence supporting or contradicting male-biased dispersal.

Here, I present a phylogeographic study of *P. subflavus* to reveal the dispersal patterns and genetic structure across the midwestern and eastern portion of the species' range (Bermingham and Moritz 1998; Rocha *et al.* 2007). I explore genetic diversity at the HV1 region of the mitochondrial genome and at eight nuclear microsatellite loci. Mitochondrial DNA (mtDNA) is inherited maternally; due to its higher mutation rate and smaller effective population size, mtDNA tends to be highly variable within and between populations, making it useful in analyzing population history (Galtier *et al.* 2009). Microsatellites are loci that consist of variable numbers of two to seven base pair tandem repeats and are used to assess variation among individuals and sampling sites (Tautz 1989; Slatkin 1995; Santana *et al.* 2009). New alleles are created through DNA slippage during replication, and the loci are typically highly variable (Slatkin 1995; Santana *et al.* 2009). Mutations at microsatellite loci are more frequent than point mutations in DNA; therefore, these loci are suitable for detecting more recent patterns of gene flow and changes in population size (Slatkin 1995). Microsatellites are inherited from both males and females; therefore, the effects of both male and female demography can be assessed by comparing mitochondrial and microsatellite data.

The goals of my study are (i) to define the geographical limits of catchment areas within the range of *P. subflavus*, (ii) to understand the dispersal patterns of both sexes, and (iii) to estimate the historical demography of *P. subflavus* populations. Given the long-distance migrations suggested by stable isotope and wind turbine data, I expect a panmictic population for *P. subflavus* (Furmankiewicz and Altringham 2007; Cryan and Barclay 2009; Fraser *et al.* 2012). Ecological studies suggest male-biased dispersal in closely related bat species (Kerth *et al.* 2002;

Arnold 2007; Chen *et al.* 2008); therefore, I predict more significant structure in the mitochondria than in the microsatellite loci, as well as higher levels of structure in the mitochondria of females than in males. Given the end of the last glacial period 15,000 years ago, I hypothesize that the historical demography of *P. subflavus* will be largely consistent with population growth, with potential recent declines due to deforestation.

METHODOLOGY

Sample Collection

Wing tissue samples from *Perimyotis subflavus* were collected from 15 locations within the species' range in the United States using the Worthington Wilmer and Barratt (1996) protocol. Sampling locations included Anderson, TN; Jackson, IL; Pendleton, WV; Pope, IL; Putnam, TN; Rowan, KY; Schuylkill, PA; Somerset, PA; Stoddard, MO; Stone, AR; Swain, NC; Vermillion, IN; Washington, MD; Wayne, IL; and Wayne, MO (Table 1, Figure 2). All samples were collected by mist netting between the months of May and August, except for Vermillion, at which site bats were captured at a maternity roost. Two three-mm wing biopsy punches from each sampled individual were stored in silica gel desiccant at 4°C. A sample size of $n \geq 5$ (average $n = 9.3$) was obtained from each site.

DNA Isolation, Fragment Analyses and Sequencing

DNA was isolated using a DNeasy isolation kit (Qiagen) following the blood and tissue protocol. To explore male behavior in comparison to female, both microsatellite and mitochondrial molecular markers were used. Mitochondrial sequences were obtained from individuals from all 15 locations and microsatellite genotypes were obtained from 14 of the 15 sites (Table 1, Figure 2). I sequenced from the non-coding HV1 region of the mitochondrial genome. The primers used were C and F from Wilkinson and Chapman (1991) with sequences: C: 5'-TGAATTGGAGGACAACCAGT-3' and F: 5'-GTTGCTGGTTTCACGGAGGTAG-3'. Illustra PuRe Taq Ready-To-Go HotStart Beads (GE Healthcare) were mixed with 0.9 mmol/L of forward primer, 0.9 mmol/L of reverse primer, 1.0 µL of DNA template, and 23 µL of H_2O for a total PCR volume of 25 µL. Cycling was performed under the following conditions: 8 min

at 96°C, 10 min at 95°C, forty cycles of 1 min at 95°C, 1.5 min at 52°C, 2 min at 72°C, and a final extension for 4 min at 72°C. PCR products were sequenced on an ABI 3130xl DNA Sequencer at Annis Water Resources Institute. A total of 140 individuals from 15 sites were sequenced (Table 1). The sequences were aligned by eye using BioEdit version 7.2.1 (Ibis Biosciences) and cropped to a common length of 587 bp.

Microsatellite markers from closely related vespertilionid species were tested on *P. subflavus* (Castella and Rueidi 2000; Piaggio *et al.* 2009b; Trujillo and Amelon 2009; Lee *et al.* 2011; Oyler-McCance and Fike 2011). The following eight microsatellite primers cross-amplified successfully and were used here: MMG9, D110, MS3E02, IBat M23, IBat CA43, Coto_F09F_F10R, Coto_G07F_G07R, and Coto_G02F_H10R (Table 2). Illustra PuRe Taq Ready-To-Go HotStart Beads (GE Healthcare) were mixed with 0.5 mmol/L of fluorescently-tagged forward primer, 0.5 mmol/L of reverse primer, 1.0 µL of DNA template, and 23 µL of H_2O for a total PCR volume of 25 µL. Cycling was performed under the following conditions: 8 min at 95°C, 2 min at 94°C, thirty cycles of 1 min at 94°C, 1.5 min at 50°C, 2 min at 72°C, and a final extension for 10 min at 72°C. PCR products were sized on an ABI 3130xl DNA Sequencer at Annis Water Resources Institute. A total of 188 individuals from 14 sites were genotyped (Table 1). Microsatellites were scored and binned in Geneious v.7.1.5 (Biomatters Limited). Genetic diversity measures including allele size range, the number of alleles observed (N_A), expected heterozygosity (H_E), and observed heterozygosity (H_O) were generated for the eight loci using GenAlEx v.6.5 (Peakall and Smouse 2012).

Population Limits

To understand the relationship between geographic distance and genetic distance based on female movement, Spearman's rank correlation test was run in R (R Development Core Team 2008) to assess the correlation between two matrices. A significantly positive correlation between transformed genetic ($F_{ST}/(1-F_{ST})$) and ln(geographic distance) matrices can imply isolation-by-distance in *P. subflavus* (Rousset 1997). Additionally, pairwise F_{ST} values were calculated in Arlquin 3.0 (Excoffier *et al.* 2007) between each sampling site to quantify population differentiation (Meirmans 2006). F_{ST} values are generated based on genetic variation between populations; low F_{ST} values (values equal to or close to zero) correspond to low levels of genetic differentiation, whereas values near or equal to one reflect populations that are genetically distinct (Wright 1931). Based on pairwise F_{ST}, sampling sites were clustered into various groupings and multiple AMOVAs were run to compare the amount of genetic variance among these groups as opposed to among the sampling sites within the groupings.

Microsatellite data were analyzed using the program STRUCTURE in which the genotypic data from individuals are clustered into *K* populations dependent upon the presence or absence of admixture (Pritchard *et al.* 2000). The true number of populations is unknown in our sampling range, therefore a range of *K* was explored from 1 (complete panmixia) to 14 (each sampling site a distinct population). Ten iterations were run for each value of *K* for 1×10^6 MCMC replications with a burn-in of 10,000. Each iteration used the admixture ancestry model and correlated allele frequencies model. Methods described by Evanno *et al.* (2005) were used to determine the most likely number of populations, *K*. ObStruct (Gayevskiy *et al.* 2014) was also used to aid in interpreting population structure. From STRUCTURE output, ObStruct uses the ancestry profiles to calculate an R^2 statistic. This R^2 statistic represents the amount of variability

that is caused by predefined populations in the data (*i.e.*, sampling locations or regions) to determine if the inferred population structure is correlated with the predefined structure set by the user. Additionally, FLOCK was used to estimate number of populations, *K* (Duchesne and Turgeon 2012). FLOCK randomly assigns genotypes into *K* groups, the number of clusters determined by the user with associated likelihood scores for each group. The genotypes are then reallocated to the cluster with the highest likelihood value. A log likelihood difference (LLOD) is reported for each run. FLOCK was run for 20 iterations for values of *K* from 1 to 14, with 50 runs per *K.* The number of clusters was determined using the plateau analysis (Duchesne *et al.* 2013).

To assess differences in dispersal patterns between the sexes, two AMOVAs were run using mitochondrial sequence data and the defined populations. One AMOVA used just female individuals (N = 64), and the other used just males (N = 75). If higher levels of structure are observed in the females than in the males, this would imply male-biased dispersal (Figure 1). Offspring inherit their mitochondrial genomes strictly through the maternal line, and not from their father. Therefore, the dispersal of females should have a greater influence on the structure of the population than male movement. If females return to their natal roost to rear offspring, then females at maternity roosts should exhibit significant population structure at mitochondrial loci, even within a catchment area. If males are the dispersing sex, then mtDNA carried by adult males should be panmictic within a catchment area because the males would disperse from the hibernaculum in any direction carrying the mtDNA from their mothers with them. If it is observed that there is higher genetic differentiation in females than in males among sampling sites, it is likely that males are the primary dispersers (O'Corry-Crow et al. 1997; Escorza-Treviño and Dizon 2000).

Effective Population Size

To estimate evolutionary parameters for both the mtDNA and nuclear data sets, the program BEAST v.1.8 (Drummond and Rambaut 2007; Drummond *et al.* 2012) was used. BEAST utilizes Bayesian Markov chain Monte Carlo (MCMC) algorithms and incorporates various evolutionary models, including clock models, tree shape models, and demographic models. Using BEAST, extended Bayesian skyline plots (Heled and Drummond 2008) were constructed for the two distinct populations detected from the mtDNA dataset. The EBSP analysis uses coalescent-based methods to reconstruct the relationship between the genealogy and the demographic history of a population (Pybus *et al.* 2000; Ho and Shapiro 2011). A coalescent event is described as the tracing of two lineages back in time to a common ancestor (Kingman 1982; Drummond *et al.* 2005). Through this reconstruction I was able to estimate the effective population size through time based on a relationship between population size and the time between coalescent events (Pybus *et al.* 2000; Ho and Shapiro 2011). In a large population, it is likely to take a longer time for two lineages to coalesce than it would for those same two lineages in a small population; therefore, variation in branch lengths through time in a genealogy can be used to infer a history of changes in effective population size (Heled and Drummond 2008). An initial analysis in jModelTest 2.1.4 (Posada 2008) indicated that the TPM1uf + G + I model best fit the mtDNA data (Kimura 1981; Darriba *et al.* 2012). The BEAST settings for the two populations were the same. These settings specified a GTR (+ Gamma + Invariant Sites) evolutionary model, a mutation rate of 10^{-5} substitutions per locus per year (Russell *et al*. 2005), with a clock rate setting of 0.017 substitutions per site per million years. All default operators were used except for three, which were altered as dem.pop.meandist (weight = 40),

dem.indicator (weight = 100), and dem.scaleActive (weight = 60) following Heled (2010). For each population, four independent BEAST runs were performed, each with a chain length of 5 x 10^8 with output logged every 25,000 steps. Results from the BEAST runs were analyzed using Tracer 1.6. Convergence was ensured by verifying that combined run effective sampling size (ESS) values were greater than 150 after a burn-in of 5 x 10^7 (10%).

MSVAR v.1.3 was used to estimate population size change over time in a single population from microsatellite data (Beaumont 1999; Beaumont 2003). The program uses MCMC simulation to estimate N_1 (effective population size at some time t in the past), N_0 (current effective population size), the time at which population size change started (Ta), and mutation rate (μ). Locus Coto_F09_F10 exhibited excess homozygosity and was therefore excluded from this analysis. Three runs of MSVAR used independent subsamples of 80 chromosomes each (N = 40 diploid individuals) from the data set of seven loci. All analyses used the same prior values (presented in $\log_{10}$ scale) for Ta (time), N_0 (current population), N_1 (ancestral population), and μ (mutation rate). Prior values for each parameter, the means of the normal distribution (α), the standard deviation of means (σ), the means of the standard deviation (β), and the standard deviations of the standard deviation (τ), were derived from suggestions by Storz and Beaumont (2002), $\alpha_{N0} = \alpha_{N1} = 7$, $\alpha_{Ta} = 4$, $\alpha_{\mu} = -5$; $\sigma_{N0} = 3.5$, $\sigma_{N1} = 4.5$, $\sigma_{Ta} = 2$, $\sigma_{\mu} = 0.5$; $\beta_{N0} = \beta_{N1} = \beta_{Ta} = \beta_{\mu} = 0$; $\tau_{N0} = \tau_{N1} = \tau_{Ta} = 0.5$, $\tau_{\mu} = 2$. The run length was 8.0 x 10^9 with parameters recorded every 10^6 steps. Convergence was assessed using the Gelman and Rubin convergence diagnostic statistic (Gelman and Rubin 1992). Higher posterior distribution intervals (95% HPD) were assessed in Tracer 1.6.

RESULTS

Summary Statistics

Considerable diversity was detected at both mitochondrial and microsatellite loci. I detected 111 distinct haplotypes out of 140 mitochondrial sequences from 15 sampling locations. Of the 587 sites, 129 were polymorphic for all sampling sites combined (Table 3). Of the 122 screened microsatellite loci, eight amplified successfully and were variable in *P. subflavus*. The number of alleles per locus ranged from 8 alleles to 37 (Table 2), with a mean of 19 alleles per locus. The mean H_0 across all sampling locations and loci was 0.790 (±0.021S.E).

Population Structure

Pairwise F_{ST} *P* values for the mitochondrial data are given in Table 4 and the relationship between genetic and geographic distance is shown in Figure 3. Sampling locations separated by large geographic distances were more genetically distinct (rho= 0.6154, $P = 2.84 \times 10^{-12}$). The results of the Mantel test and the pairwise F_{ST} analyses were used to define populations within *P. subflavus'* range. Locations that were genetically similar were clustered together. Different sets of groupings were analyzed by AMOVA, and the populations were resolved by the pattern that minimized variance among locations within groups (ϕ_{SC}) and maximized variance among groups (ϕ_{CT}). The mitochondrial sequence data support two subpopulations across the sampled range of *P. subflavus* (Table 4, Figure 4). Population one (referred to as "West") clustered Anderson, TN; Jackson, IL; Pope, IL; Putnam, TN; Rowan, KY; Stoddard, MO; Stone, AR; Swain, NC; Vermillion, IN; Wayne, IL; and Wayne, MO. Population two (referred to as "Appalachian") included Pendleton, WV; Schuylkill, PA; Somerset, PA; and Washington, MD. The AMOVA results revealed that more genetic variation is due to differences between groups of sampling

sites (ϕ_{CT}: 22.45% variation, $P = 0.0007$) than among sampling sites within groups (ϕ_{SC}: 9.23% variation, $P < 0.00001$; Table 5). The Appalachian population had 29 haplotypes, and West had 92 haplotype (Table 3).

Analyses of population structure at the microsatellite loci revealed a panmictic population. Pairwise F_{ST} values show no significant genetic differentiation among locations (*P* values in Table 6). Multiple evaluations of the STRUCTURE results similarly support a single panmictic population from the nuclear microsatellite data (Figure 5). Figure 5A illustrates the Evanno *et al.* (2005) method of evaluating ΔK. Here, the most likely value of *K* is determined by a peak or plateau in the graph of ΔK. Though the observed peak in ΔK is at $K = 2$, the Evanno *et al.* (2005) method cannot evaluate the case of $K = 1$. The mean lnP(*K*) values from STRUCTURE, however, suggest that the most likely number of clusters is one (Table 7). The STRUCTURE results were also evaluated using ObStruct, which reveals correlations between predefined populations (sampling locations) and inferred populations (Gayevskiy *et al.* 2014). The canonical discriminant analysis (CDA) uses ancestry files created by STRUCTURE and transforms the data to fit two variables. The two best variables from the CDA together explain around 54.79% (16.87%, 37.92%) of the variability (Figure 5B). The graph shows the median and the 50% ellipsoid for each pre-defined sampling location. There is no clear clustering of individuals to indicate the presence of more than one population (Figure 5B). The CDA does indicate that there is variability within pre-defined sites, such as locations 3 (Somerset, PA) and 11 (Jackson, IL). Results from FLOCK show no plateaus of LLOD values for any value of $K > 1$, suggesting a panmictic population (Table 8).

Results of the AMOVAs based on sex showed more structure in the mitochondria of females than of males (Table 9). There was more structure observed between the Appalachian

and West populations based on genetic differentiation in females (ϕ_{ST} = 0.5738) than in males (ϕ_{ST} = 0.2363), but both were significant ($P < 0.0001$). Higher levels of genetic differntiation were also observed in the mitochondria of females within a catchment area (ϕ_{SC}= 0.1518, P = 0.0019) than in males (ϕ_{SC} = 0.0865, P = 0.0356).

Population Demography Inference

Coalescent extended Bayesian skyline plots (EBSP) were used to estimate the magnitude and timing of female effective population size changes in the Appalachian and West populations (Figure 6, Figure 7). Both Appalachian and West experienced population size increases starting around 14,760 (13,474 - 16,046) and 28,090 (25,669 - 30,505) years ago, respectively. The current female effective population sizes averaged across four BEAST runs for Appalachian and West were 390,000 (95% HPD 0.006 – 7.82 x 10^6) and 386,000 (95% HPD 0.015 – 4.30 x 10^6), respectively (Table 10). The ancestral size of the Appalachian population was 10,300 (±76.1 S.E.) females, and the ancestral size of the West was 19,400 (±77.1 S.E.) (Table 10).

Runs in MSVAR unanimously showed population size decrease within the single panmictic population described from the microsatellite data (Figure 8, Table 11). Across three runs, the ancestral effective population size (N_1) was estimated at around 3.13 million (95% HPD: 0.027 – 3.49 x 10^7), with point estimates from individual runs ranging from 2.06 to 6.51 million individuals. This ancestral population decreased to a current effective population size (N_0) of 9,262 individuals (95% HPD: 0.00001 – 3.78 x 10^6), with run estimates ranging from 760 - 15,700 individuals. The estimated start of this decline was approximately 1,000 years ago (95% HPD: 0.00003 – 3.85 x 10^5). The maximum ratio of N_0/N_1 was 0.664 with a combined value across runs of 0.611.

DISCUSSION

The eastern pipistrelle bat (*Perimyotis subflavus*) is subject to three major conservation threats: habitat loss, white-nose syndrome mortality, and wind turbine fatality. In recent years, studies have revealed that *P. subflavus* has shown negative responses to forest fragmentation (Farrow and Broders 2011), experienced similar rates of mortality from white-nose syndrome as *Myotis lucifugus* (O'Connor *et al.* 2011), and is one of the more heavily affected of the 21 bat species killed at wind turbines in North America (Cryan and Barclay 2009). With a range that covers most of eastern and central North America (Fujita and Kunz 1984), it is essential to discern the geographic limits and movements of populations of this species to better understand which populations may be at higher risks. However, population limits and genetic structure of *P. subflavus* had been largely undocumented prior to this study. Rising threats to bats such as habitat destruction and fragmentation (Fuentes-Montemayor *et al.* 2013), white-nose syndrome (Reeder and Moore 2013), and wind energy (Arnett and Baerwald 2013) make population connectivity and effective population size estimates increasingly useful in conservation management decision making.

Genetic Structure and Sex-biased Dispersal

Gene flow among populations contributes significantly toward maintaining genetically variable and sustainable populations (Segelbacher *et al.* 2009). Phylogeographic studies have revealed different levels of structure and connectivity in various species of bats (Rivers *et al.* 2005; Chen *et al.* 2006; Lu *et al.* 2013). The extent to which bat populations are connected is determined primarily by the dispersal capabilities of the organism rather than the permeability of the matrix surrounding sustainable habitat. In temperate bat species, it is common for males to

disperse while females exhibit site fidelity, though some female dispersal does occur on a local scale (Moussy *et al.* 2013). Additionally, population structure in hibernating temperate bat species can be complicated by the fact that mating occurs promiscuously during fall swarming at sites in which individuals from large portions of the summer range may be collected. In this study, I examined both mitochondrial and microsatellite markers to assess genetic structure across the eastern range of *P. subflavus*.

Across 14 locations within the range of *P. subflavus*, there was very little genetic differentiation revealed by pairwise F_{ST} values in the nuclear markers (Table 6). However, the Mantel test and analyses of molecular variance of mtDNA data from 15 locations revealed significant structure across the sampled range (Figure 3, Table 5). This observed pattern of significant structure in maternally inherited markers with a lack of structure in nuclear markers is often associated with male-biased dispersal (Prugnolle and de Meeus 2002), but additional analyses are required in migratory species (Figure 1). Sex-segregated AMOVAs show higher levels of mitochondrial structure in females than in males (Table 9). This suggests male-biased dispersal in *P. subflavus*, which is consistent with the pattern inferred in many other vespertilionids (*Myotis bechsteinii*, Kerth *et al.* 2002; *Corynorhinus* spp., Piaggio *et al.* 2009a; *Eptesicus fuscus*, Turmelle *et al.* 2011; *Myotis lucifugus*, Miller-Butterworth *et al.* 2014); however, to test this more directly, additional analyses with paternally inherited markers are required.

Eastern pipistrelles are considered regional migrants, and are capable of up to 500 km movements between their summer and winter roost (Fleming and Eby 2003), but most banding studies suggest they are likely to move less than 140 km (Griffin 1940; Barbour and Davis 1969; Fujita and Kunz 1984). However, recent stable isotope data have shown that male *P. subflavus*

are making latitudinal movements similar to those associated with long distance migrating bat species, such as hoary bats (*Lasiurus cinereus*), eastern red bats (*Lasiurus borealis*), and silver-haired bats (*Lasionycteris noctivagans*, Fraser *et al.* 2012). Mortality of this species at wind turbines also suggests they may be migrating longer distances than previously thought (Cryan and Barclay 2009). My results demonstrating a lack of genetic structure among eastern and western sites at nuclear loci further suggests that males may be moving farther distances on a longitudinal scale, which is a directional aspect that could not be assessed with the stable isotope data.

While the nuclear data indicate that males are capable of long distance movements, comparisons with mitochondrial data suggest that females are making shorter distance dispersals. Although clustering patterns based on pairwise F_{ST} estimates for mtDNA were ambiguous (Table 4), the use of AMOVAs helped to determine appropriate groupings (Table 5). The division of sampling sites into Appalachian and West regions resulted in clear genetic differentiation among those regions, but not complete (22.45% variance between regions). Sampling sites that were geographically distant but within the same region remained genetically similar. In the terms of an AMOVA, this clustering pattern maximized ϕ_{CT} while minimizing ϕ_{SC}. This pattern revealed some violations of a strict isolation-by-distance model. For example, samples from Schuylkill, PA, and Pendleton, WV, were genetically similar enough to group within the Appalachian population despite being more than 400 km apart (pairwise $F_{ST} = 0.0244$, $P = 0.2383$). This suggests that females may be exhibiting more of a "regional" fidelity than site fidelity (Vonhof *et al.* 2008). The only exception to this was location 15 (Vermillion, IN), which was a maternity roost, and was genetically distinct from all other sites regardless of geographic distance. Although the individuals from Vermillion, IN, were significantly genetically distinct, there were

haplotypes shared with locations in the West population (n_h= 4, shared h= 2), supporting some low but non-negligible intra-regional female dispersal.

Geographic landscape features may also contribute to the genetic structure detected in females. For example, the Appalachian Mountain range separates the eastern sites of the Western population from the western sites of the Appalachian population. Latitudinal movements may allow for gene flow among sites within each population, but limit exchange of females between populations. To get a better understanding of geographical limits for this population would require additional sampling. Though sites represented here cover a large portion of the species' range, there are gaps between some sites, as well as entire regions that went un-sampled (northeast, northern midwest, southeast, southwest). Filling in the range of the eastern pipistrelles with additional sampling locations would help researchers understand the extent to which the females are capable of dispersing.

Effective Population Size and Population Size Change

Past population size changes were inferred for both mitochondrial populations and in the microsatellite data. However, there was a discrepancy between patterns inferred from the two marker types. Analyses of microsatellite data suggest a very recent population decrease, while EBSP analyses of mitochondrial data suggest this decline was preceded by population growth farther back in time.

The time of population growth reconstructed from mitochondrial data roughly corresponds with the end of the last glacial period (~15,000 years ago). Appalachian and West populations show an increase in female effective population size (N_{ef}) from ancestral effective

population sizes (N_1) of approximately 10-20,000 females to current effective population sizes (N_0) of 390,000 females, respectively, between 15-28,000 years ago (Table 10).

In the panmictic population described from microsatellite loci, there was a population size difference in N_0 when compared to the mitochondrial results. Effective population size estimates from microsatellite data were an order of magnitude smaller compared with mitchondrial data. Additionally, there was a severe population decline supported by the microsatellites while mitochondrial data suggest a population increase. The current effective population size (N_0) estimated across three runs of microsatellite data was approximately 9,000 individuals, while the ancestral effective population size N_1 was estimated to be about 3.1 million. This population decline was estimated to start around 1,000 years ago (Table 11). This suggests the population experienced a large bottleneck quite recently in the species' evolutionary history, possibly corresponding with the early stages of climate change.

Such strong variation in the results from mitochondrial and microsatellite data are in part due to the differences in the underlying methodologies in either program and the nature of the markers. The more recent population size change reconstructed from the microsatellite data is a byproduct of the sensitivity of these markers to recent demographic events due to the fast mutation rate of microsatellite loci. The discrepancy between markers for effective population size is more likely due to large variability in the posterior distributions. BEAST used mitochondrial data to estimate the effective female population size. For this value to be comparable to the overall size estimated by the nuclear data, the mitochondrial N_e values must be doubled (assuming the sex ratio is equal). However, this adjustment only intensifies the gap between the N_e estimated by mitochondrial and microsatellite data. The range of the posterior distribution of both estimates is quite large (Table 10, Table 11, Figure 9), and most variability in

both the nature of the population size change (increase or decrease) and the point estimate of N_0 can be attributed to this. Additional sampling in surrounding areas may give a more accurate representation of the effective population size for this region.

Conservation and Management

Threats to biodiversity are on the rise, with current estimated extinction rates between 100-1000 times higher than those observed in the past, averaging 100 extinctions per million species-years (Pimm *et al.* 1995; Pimm *et al.* 2014). Major threats to biodiversity include invasive species, habitat loss and fragmentation, climate change, and disease (Pimm *et al.* 1995; Smith *et al.* 2009). Emerging infectious diseases (EID) are those that are newly discovered in a population, have recently inhabited a new host, or have already existed and are increasing in prevalence or geographic dispersal (Daszak *et al.* 2001; Williams *et al.* 2002).

North American insectivorous bats are under tremendous conservation pressure. New threats, including the EID known as white-nose syndrome and the increase in use of wind energy have threatened the sustainability of several species, and the result could span trophic levels (Arnett *et al.* 2010; Cryan *et al.* 2010). If conserving bats for the sake of species diversity is not enough, insectivorous bats are also of great economic value. In North America, insectivorous bats control many crop-feeding insect populations (Boyles *et al.* 2011). A decline in these populations could lead to agricultural losses of more than $3 billion/year (Boyles *et al.* 2011). A key factor in understanding population extinction risk is knowing how many individuals constitute a population.

Estimating values of effective population size (N_e) is useful but it is less informative for conservation and management efforts than census size (N_C). Effective population size is

described as the number of individuals that would be required in an ideal Wright-Fisher population to yield the same level of diversity as what is observed in a sampled population (Fisher 1930; Wright 1931; Luikart *et al.* 2010). Census size is the actual number of adults in the population (Luikart *et al.* 2010). A populations' census size is difficult to quantify and any method short of counting each individual is subject to misrepresenting the actual value. Bats are particularly hard to observe, and counting methods can be subject to considerable error. They roost in difficult-to-access locations such as caves, foliage, tree cavities, and crevices in man-made structures (Kunz *et al.* 2009). Commonly used methods for estimating N_C in bats include roost counts, emergence counts, acoustic recordings, and mark-recapture studies, but each has particular limitations (Kunz *et al.* 2009). However, effective population size estimates have limitations, too. In coalescent methods, as seen here, the amount of error in the posterior distribution or likelihood surface can make it difficult to draw definitive results. In other cases, recent population declines may go undetected in molecular methods until the population has already become very small (Vonhof and Russell 2013).

There is the potential to infer N_e from N_C and vice versa using the N_e/N_C ratio. The effective population size is usually smaller than the census size, averaging between 10-50% of the census size for most species (Hare *et al.* 2011). However, the N_e/N_C ratio is likely to change over time in species with variable life histories (Luikart *et al.* 2010). For example, several long-term studies documented the variation of this ratio over time in steelhead trout, red flour beetles, salmonids, and frog species due to fluctuating reproductive success, effects of immigration on N_e, and variability in the effect of census size on N_e/N_C ratio (high N_C in salmonids led to a higher N_e/N_C ratio, while high N_C in red flour beetle had the opposite effect, Luikart *et al.* 2010). The average N_e/N_C ratio across a range of species when excluding life history variables is 0.34,

but comprehensive estimates including said variables resulted in an average ratio of 0.11 (Frankham 1995). Across mammal species, the N_e/N_C average ratio is 0.46 (Frankham 1995).

While management efforts may focus on N_C, effective population size still has valuable applications of its own. The value of N_e can be used to assess a population's ability to adapt and persist after stochastic events (Hare *et al.* 2011), such as high mortality from a novel pathogen or decreased yearling survival due to climate change. Such stochastic events contribute to genetic drift, the random loss of alleles from a population due to individual mortality or lack of reproduction. As the value of N_e decreases, the effect of genetic drift on the population increases. The disappearance of alleles from a population decreases the overall genetic diversity, which increases the chance of allele fixation and inbreeding, and lessens the effect of natural selection (Hare *et al.* 2011; Heller *et al.* 2010). N_e can be used to predict future genetic diversity under various demographic scenarios. This is useful in that it allows researchers to assess the health of a given population without knowing the census size. Sub-sampling can be done within a species' range, and the species can be considered at risk or healthy based on the N_e estimated from samples as compared to the simulated N_e required to maintain a healthy level of genetic diversity.

CONCLUSION

Recent threats to temperate bat species have heightened the need to preserve genetic diversity. My results suggest that the eastern pipistrelle population has been on the decline for the last 1,000 years; with white-nose syndrome and wind turbine mortality, the species is experiencing additional unexpected mortality. To maintain a healthy population despite these declines, genetic diversity must be maintained in the eastern pipistrelle population.

The presence of genetically differentiated populations in this migratory, swarming bat species indicates the importance of catchment areas in genetic diversity. This calls for the management and protection of both hibernacula and swarming locations which promote gene flow among individuals from isolated summer locations. Additionally, the movement capabilities of both males and females present the need for wind farm regulation during the peaks of the fall and spring migratory seasons in order to lessen the effect on long-distance migratory species.

Figure 1

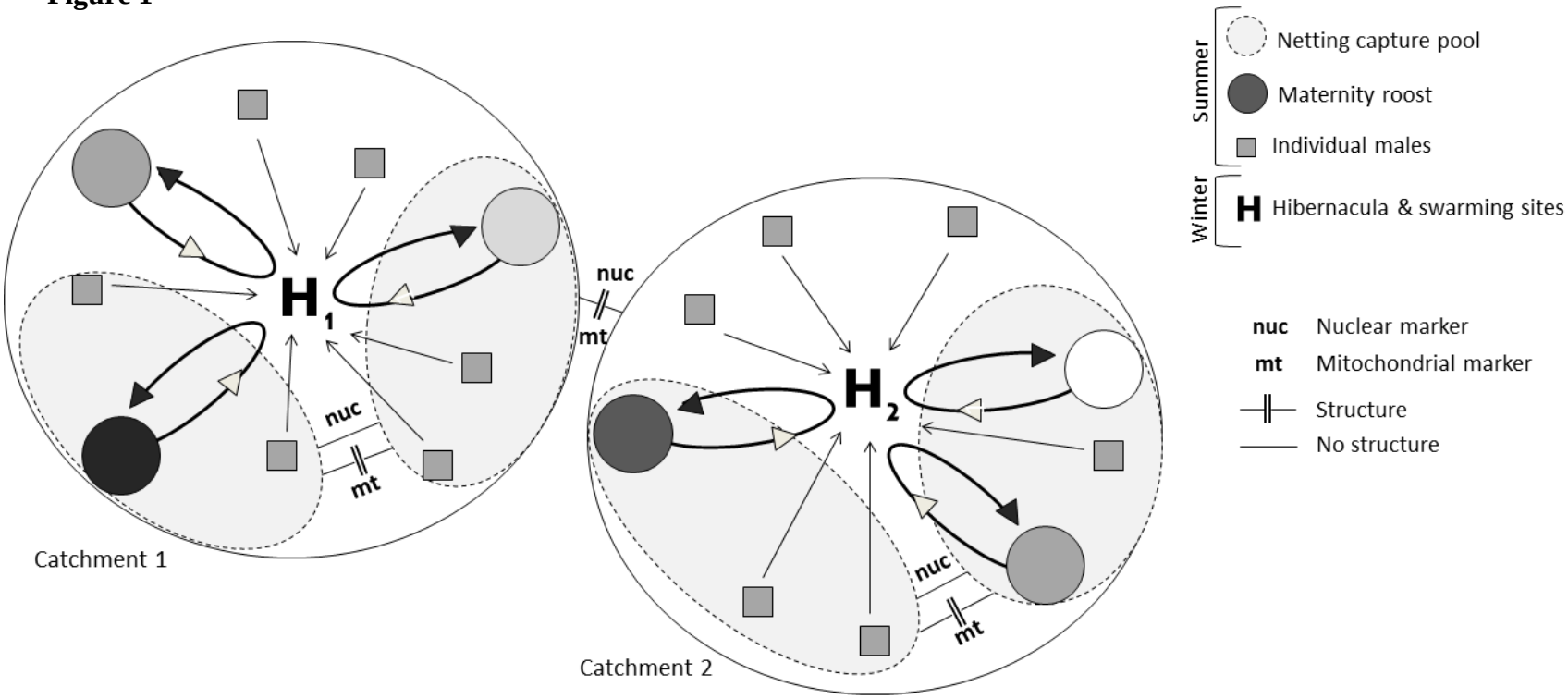

Figure 1. Genetic structure expected based on the movement and behaviors of migratory temperate bat species. There is no predicted structure in the nuclear DNA among sampling pools within a catchment area, while there is predicted structure in the mitochondrial DNA. Additionally, there is expected to be more mitochondrial structure among females than males within a catchment area. Alternatively, there is predicted structure at both nuclear and mitochondrial loci among catchment areas, regardless of sex.

Table 1 Coordinates and sampling sizes for fifteen *P. subflavus* sampling locations. For each location, N represents the number of individuals sampled for either marker. The average number of individuals genotyped across eight microsatellite loci is used as N (total number sampled). Putnam, TN (site 8) was not genotyped at microsatellite loci.

Location ID	Location (County, State)	Coordinates		mtDNA N	Average Microsatellite N across Loci
1	Schuylkill, PA	40.7000 N	76.2100 W	10	19.0 (19)
2	Washington, MD	39.6000 N	77.8100 W	10	13.8 (14)
3	Somerset, PA	39.9700 N	79.0300 W	5	3.9 (5)
4	Pendleton, WV	38.6800 N	79.3600 W	9	14.8 (15)
5	Rowan, KY	38.1900 N	83.4200 W	12	16.9 (17)
6	Anderson, TN	36.1950 N	84.0400 W	10	14.3 (15)
7	Swain, NC	35.4900 N	83.4900 W	9	12.6 (13)
8	Putnam, TN	36.1400 N	85.5000 W	6	-
9	Wayne, IL	38.4194 N	88.6472 W	8	4.9 (5)
10	Pope, IL	37.4091 N	88.6622 W	11	19.1 (20)
11	Jackson, IL	37.7900 N	89.3800 W	9	7.3 (8)
12	Stoddard, MO	36.8600 N	89.9500 W	10	12.9 (13)
13	Wayne, MO	38.4194 N	77.8100 W	10	13.6 (14)
14	Stone, AR	35.8794 N	92.1472 W	9	19.0 (20)
15	Vermillion, IN	39.8500 N	87.4600 W	12	9.8 (10)

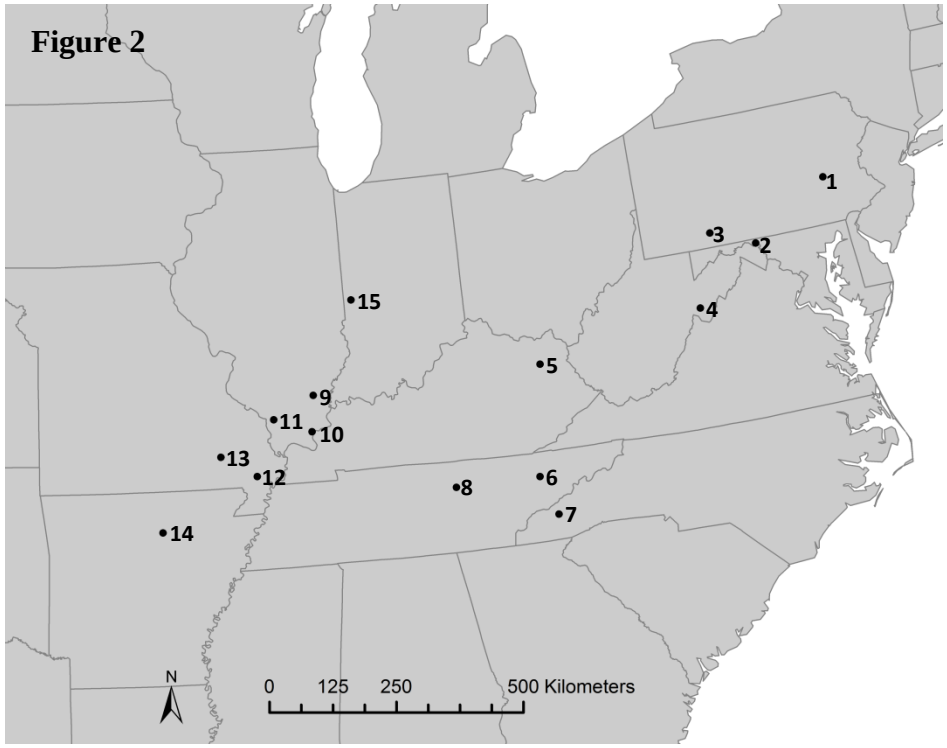

Figure 2. Fifteen sampling locations for *P. subflavus* wing tissue. Wing tissue was collected from fifteen locations in total. Samples from one site (site 8) were only utilized for the collection of mitochondrial data, resulting in 15 locations for mitochondrial sequence and 14 locations for microsatellite data. Location numbers correspond with Table 1.

Table 2. Characteristics of eight microsatellite loci developed in closely related vespertilionid species that successfully amplified in *P. subflavus*. The forward sequences were tagged with fluorescent dyes ([1]NED, [2]VIC, [3]PET). Data specific to *P. subflavus* are displayed for each primer pair, including allele size range, the number of alleles produced (N_A), expected heterozygosity (H_E), and observed heterozygosity (H_O) (± standard error).

Primer name	Primer sequence	Repeat motif	Allele size range (bp)	N_A	H_O	H_E	Reference
MMG9	[1]F: AGGGGACATACAAGAATCAACC	$(TC)_{19}$	124-184	25	0.945	0.883	Castella and Ruedi
	R: TAATTTCTCCACTGAACTCCCC				±0.02	±0.01	2000
D110	[2]F: AGCCTCCATGATTACATAAGC	TAGA	185-233	12	0.921	0.812	Lee *et al.* 2011
	R: ACGATGCTTTTAACCTCTGAG				±0.02	±0.02	
MS3E02	[3]F: GCCAATAAGAGCCCAGACATAC	$(AC)_{22}$	364-404	19	0.842	0.804	Trujillo and
	R: GGGGATTAGGGATAGGTTAGCA				±0.05	±0.02	Amelon 2009
IBat M23	[1]F: ATCCTGGGTTTTGGGTTCAT	$(GATA)_{14}$	107-211	8	0.399	0.430	Oyler-McCance
	R: TCATGTAAATTTCAAAAACAGCAAA				±0.04	±0.02	and Fike 2011
IBat CA43	[3]F: TGC AGT CAT CTC AGC CTG TC	Di-repeat	185-251	11	0.582	0.608	Oyler-McCance
	R: TTG GTG AGA GGC TCT GCT TT				±0.04	±0.02	(un-published)
Coto_F09F_F10R	[2]F: GAGAAGGAAGAGAAACTGGTGTT	$(AC)_{23}$	165-215	21	0.846	0.850	Piaggio *et al.*
	R: TACTAAAGAACCTTGACAGTGGC				±0.03	±0.10	2009b
Coto_G07F_G07R	[1]F: GATGAAGATTCAGCTTATGATGC	$(GT)_9$	328-374	19	0.856	0.809	Piaggio *et al.*2009b
	R: AGCCCTCTATTTCATACCACAGT				±0.05	±0.02	
Coto_G02F_H10R	[2]F: AGAGTGCTTTTATGGGCAAAT	$(GT)_{20}$	133-291	37	0.926	0.884	Piaggio *et al.*2009b
	R: TGCTTGTAGTTCCCTTTCCTT				±0.03	±0.01	

Table 3. Summary of variability in the HV1 region of the mitochondrial D-loop for two *P. subflavus* populations. N, sample size; n_h, number of haplotypes; U*h*, number of unique haplotypes within population (only one present within population); S, number of segregating sites; π, nucleotide diversity.

Population	N	n_h	U*h*	S	π
Appalachian	34	29	26	39	0.01601 ± 0.0084
West	106	92	82	119	0.01846 ± 0.0094
Combined	140	111	98	129	0.01992 ± 0.0101

Table 4. Pairwise F_{ST} P values and corresponding ln(geographic distance) for mitochondrial sequence data from fifteen locations. Location numbers correspond to the ID in Table 1. The left portion of the matrix represents the P values correlated with pairwise F_{ST} values. The alpha value was corrected via Bonferroni correction, resulting in an adjusted alpha value of $\alpha = 0.00357$. Significant values are in bold. The right side of the matrix shows the ln(distance (km)) for each pair of locations. The dotted lines encasing sampling locations 1 through 4 represent the Appalachian population. The dotted line encasing locations 5 through 15 represent the West population.

	1	2	3	4	5	6	7	8	9	10	11	12	13	14	15
1	*	5.3356	5.6727	6.0495	6.7470	6.8973	6.9382	7.0124	7.1390	7.1876	7.2323	7.3094	7.3487	7.5186	6.9901
2	0.0631	*	5.0760	5.4196	6.4819	6.6737	6.7206	6.8158	7.0283	7.0787	7.1286	7.1679	7.2317	7.4049	6.8490
3	0.9346	0.1670	*	5.2242	6.3297	6.7385	6.7826	6.8721	6.8801	6.9443	7.0011	7.1165	7.1442	7.3154	6.6826
4	0.2383	0.0078	0.3750	*	6.2341	6.5317	6.5866	6.6994	6.8850	6.9497	7.0054	7.0473	7.1162	7.2868	6.8107
5	**<0.0001**	**<0.0001**	0.0410	0.0107	*	5.8090	6.1779	5.8432	6.1587	6.2876	6.3942	6.4695	6.5893	6.8637	6.2600
6	0.0049	0.0049	0.0479	0.0068	0.2207	*	5.2242	4.9812	6.4680	6.2900	6.4059	6.4267	6.5514	6.7724	6.5431
7	0.2334	0.0147	0.4971	0.6709	0.0606	0.0859	*	5.6245	6.6712	6.5580	6.6469	6.6637	6.7659	6.9349	6.7362
8	**0.0029**	**0.0010**	0.0127	0.0059	0.1943	0.6123	0.0879	*	6.1872	5.9876	6.1395	6.1793	6.3366	6.5955	6.4019
9	**<0.0001**	**<0.0001**	0.0059	**<0.0001**	0.0527	0.1406	0.0215	0.2520	*	4.8222	5.0041	5.6440	5.9217	6.3499	5.5160
10	**<0.0001**	**<0.0001**	**0.0020**	**0.0029**	0.1182	0.2969	0.0137	0.6289	0.2910	*	4.6730	5.1708	5.5535	6.1440	5.7880
11	**<0.0001**	**<0.0001**	0.0078	**0.0010**	0.0205	0.0430	0.0107	0.1162	0.9082	0.1387	*	4.9054	5.1898	6.1067	5.8888
12	0.0049	**<0.0001**	0.0430	0.0127	0.0440	0.0957	0.2305	0.1670	0.1221	0.1065	0.0654	*	4.5466	5.7117	6.1863
13	**0.0029**	**<0.0001**	0.0205	**0.0010**	0.0908	0.1221	0.0527	0.3281	0.4404	0.2588	0.2607	0.2813	*	5.6853	6.2636
14	**<0.0001**	**<0.0001**	0.0059	**<0.0001**	0.0176	0.0381	0.0233	0.0996	0.2813	0.0322	0.1006	0.2627	0.3018	*	6.6527
15	**<0.0001**	**<0.0001**	**<0.0001**	**<0.0001**	**0.0010**	**<0.0001**	**<0.0001**	**<0.0001**	**<0.0001**	**<0.0001**	**<0.0001**	**<0.0001**	**0.0010**	**<0.0001**	*

Figure 3

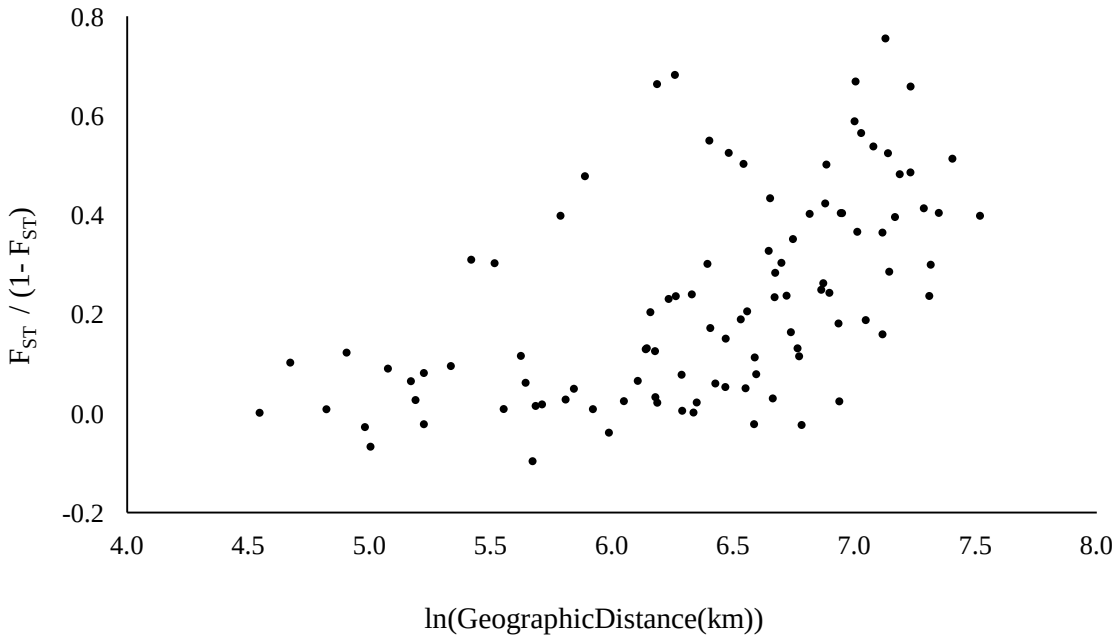

Figure 3. The relationship between genetic distance and geographic distance for *P. subflavus* sampling locations. Locations that are farther away geographically tend to be more distinct genetically from each other. Some of the genetic differentiation can be explained partially by the geographic distance (rho= 0.6154).

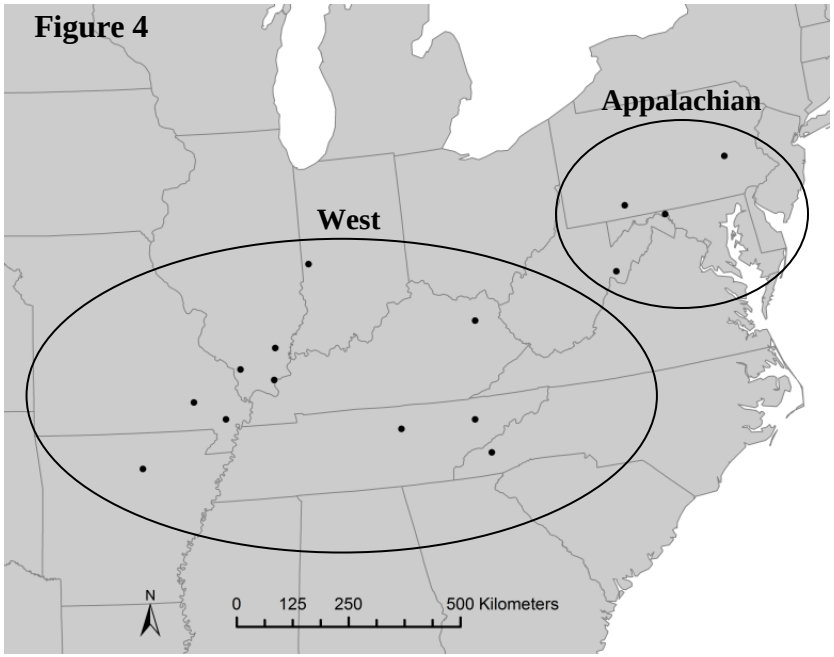

Figure 4. Sub-structuring into two populations within the range of *P. subflavus*. Based on pairwise F_{ST} values estimated from mitochondrial sequences, the sampling sites were clustered into two groups: West and Appalachian. This grouping separated significantly differentiated sites (F_{ST} *P* value < 0.00357), while minimizing variation among sites within each group (AMOVA variation resulting from differences among sites within groups ϕ_{SC} = 9.23%, and variation resulting from differences between groups ϕ_{CT} = 22.45).

Table 5. Results of the AMOVA for two populations within *P. subflavus'* range based on mtDNA sequence data.

	Sum of Squares	Variance Component	Percent of Variation	Fixation Indices	*P* value
Among Groups (ϕ_{CT})	89.77	1.5392	22.45%	0.2245	0.00070 ± 0.00012
Among Sampling Locations within Groups (ϕs_C)	137.52	0.6327	9.23%	0.1190	<0.00001 ± 0.00000
Within Sampling Locations (ϕ_{ST})	585.68	4.6854	68.33%	0.3167	<0.00001 ± 0.00000

Table 6. Pairwise F_{ST} *P* values and corresponding ln(geographic distance) for fourteen locations for eight microsatellite loci. The left portion of the matrix represents the *P* values correlated with pairwise F_{ST} values. The alpha value was corrected via Bonferroni correction, resulting in an adjusted alpha value of $\alpha = 0.00385$. The right side of the matrix shows the ln(geographic distance (km)) for each pair of locations. The location value corresponds to Table 1; there is no genotypic data for location 8, Putnam, TN.

	1	2	3	4	5	6	7	9	10	11	12	13	14	15
1	*	5.3356	5.6727	6.0495	6.7470	6.8973	6.9382	7.1390	7.1876	7.2323	7.3094	7.3487	7.5186	6.9901
2	0.0811	*	5.0760	5.4196	6.4819	6.6737	6.7206	7.0283	7.0787	7.1286	7.1679	7.2317	7.4049	6.8490
3	0.9910	0.9820	*	5.2242	6.3297	6.7385	6.7826	6.8801	6.9443	7.0011	7.1165	7.1442	7.3154	6.6826
4	0.2703	0.2252	0.9910	*	6.2341	6.5317	6.5866	6.8850	6.9497	7.0054	7.0473	7.1162	7.2868	6.8107
5	0.5225	0.6216	0.9910	0.8288	*	5.8090	6.1779	6.1587	6.2876	6.3942	6.4695	6.5893	6.8637	6.2600
6	0.5045	0.8919	0.9820	0.9099	0.9820	*	5.2242	6.4680	6.2900	6.4059	6.4267	6.5514	6.7724	6.5431
7	0.1622	0.8108	0.9820	0.4054	0.7387	0.3964	*	6.6712	6.5580	6.6469	6.6637	6.7659	6.9349	6.7362
9	0.5496	0.6126	0.9639	0.7658	0.5586	0.4865	0.7207	*	4.8222	5.0041	5.6440	5.9217	6.3499	5.5160
10	0.0631	0.3604	0.9910	0.9640	0.6216	0.7478	0.4865	0.7748	*	4.6730	5.1708	5.5535	6.1440	5.7880
11	0.1081	0.1351	0.8018	0.1171	0.1141	0.1802	0.1351	0.4144	0.0631	*	4.9054	5.1898	6.1067	5.8888
12	0.0631	0.3333	0.9910	0.4685	0.5496	0.5045	0.9460	0.5225	0.1081	0.1802	*	4.5466	5.7117	6.1863
13	0.2162	0.5045	0.9550	0.2973	0.1982	0.4054	0.4324	0.7117	0.3514	0.3063	0.1802	*	5.6853	6.2636
14	0.3874	0.4505	0.9730	0.4865	0.5586	0.5135	0.5225	0.6757	0.6126	0.1441	0.2072	0.6757	*	6.6527
15	0.0090	0.2883	0.8469	0.1802	0.2883	0.3964	0.2883	0.2162	0.0451	0.0360	0.0360	0.0360	0.2703	*

Figure 5

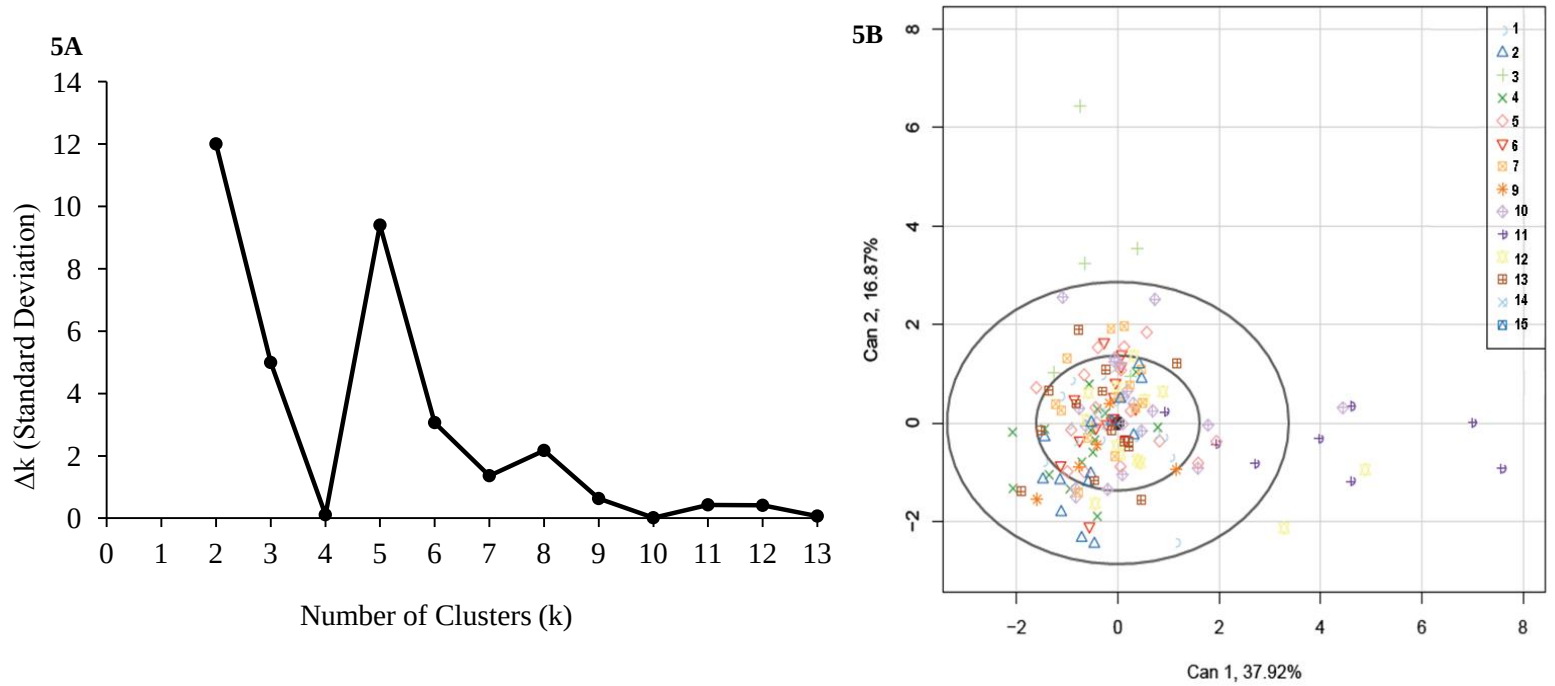

Figure 5. Estimation of the number of populations, *K*, based on Δ*K* and canonical discriminant analyses. A. Evanno *et al.* (2005) identified the most likely value of *K* using several graphical methods. Shown here is the method by which the relative support for different *K* values is assessed using Δ*K*. The value at which *K* peaks is the most likely value of *K*, shown here at *K*=2. However, this method is not informative for *K*=1. B. ObStruct canonical discriminant analysis (CDA) results for the STRUCTURE runs show that there is no apparent clustering of individuals into more than one population. The CDA also shows that sampling locations 3 (Somerset, PA) and 11 (Jackson, IL) have variability within the sampling location.

Table 7. The mean lnP(*K*) across ten STRUCTURE runs for *K* values 1 through 14. Calculations to estimate Δ*K* follow the Evanno *et al.* (2005) method. The values of Δ*K* are graphed in Figure 4A.

K	Mean LnP(*K*)	Stdev LnP(*K*)	Ln'(*K*)	|Ln"(*K*)|	Delta *K*
1	-6726.8	0.5	-	-	-
2	-7102.3	47.7	-375.6	572.28	12.0
3	-6905.6	50.6	196.7	252.71	5.0
4	-6961.6	42.6	-56.0	4.75	0.1
5	-7012.8	62.0	-51.24	582.43	9.4
6	-7646.5	108.2	-633.67	331.9	3.1
7	-7948.3	261.4	-301.77	356.2	1.4
8	-7893.8	134.0	54.4	291.22	2.2
9	-8130.6	217.1	-236.79	136.86	0.6
10	-8230.6	232.1	-99.93	3.4	0.0
11	-8333.9	281.5	-103.33	120.73	0.4
12	-8316.5	177.1	17.4	73.02	0.4
13	-8372.1	209.0	-55.62	14.41	0.1
14	-8413.3	181.0	-41.21	-	-

Table 8. Mean log likelihood difference (LLOD) and length of LLOD plateau for 50 runs of each *K* value, from 2 to 14. Consistency across runs for the same value of *K* results in identical LLOD values. Multiple identical LLOD values are known as "plateaus". The value of *K* at which the longest chain of plateaus is observed is the most likely value of *K*. Absence of plateaus for any value of *K* is indicative of lack of structure. After four consecutive *K* values in which no LLOD plateaus are attained, FLOCK terminates. FLOCK results indicate there is one panmictic population based on nuclear data.

K	Mean LLOD	*P* value	Plateau Length	Completed Runs	Aborted Runs
1	-	-	-	-	-
2	2.218888	0.250371	0	50	0
3	2.076545	0.230949	0	50	0
4	2.116954	0.399615	0	50	0
5	2.160701	0.464576	0	50	0
6	2.110808	0.545575	0	45	5
7	1.990507	0.132867	0	15	35
8	-	-	-	0	50
9	-	-	-	0	50
10	-	-	-	0	50
11	-	-	-	0	50
12	-	-	-	0	50
13	-	-	-	0	50
14	-	-	-	0	50

Table 9. Results from two sex-specific AMOVAs using mitochondrial sequences for Appalachian and West populations.

Population	ϕ_{ST}	*P* values	ϕ_{SC}	*P* values
Appalachian-West				
Female	0.5738	< 0.0001	0.1518	0.0019
Males	0.2363	< 0.0001	0.0865	0.0356

Figure 6

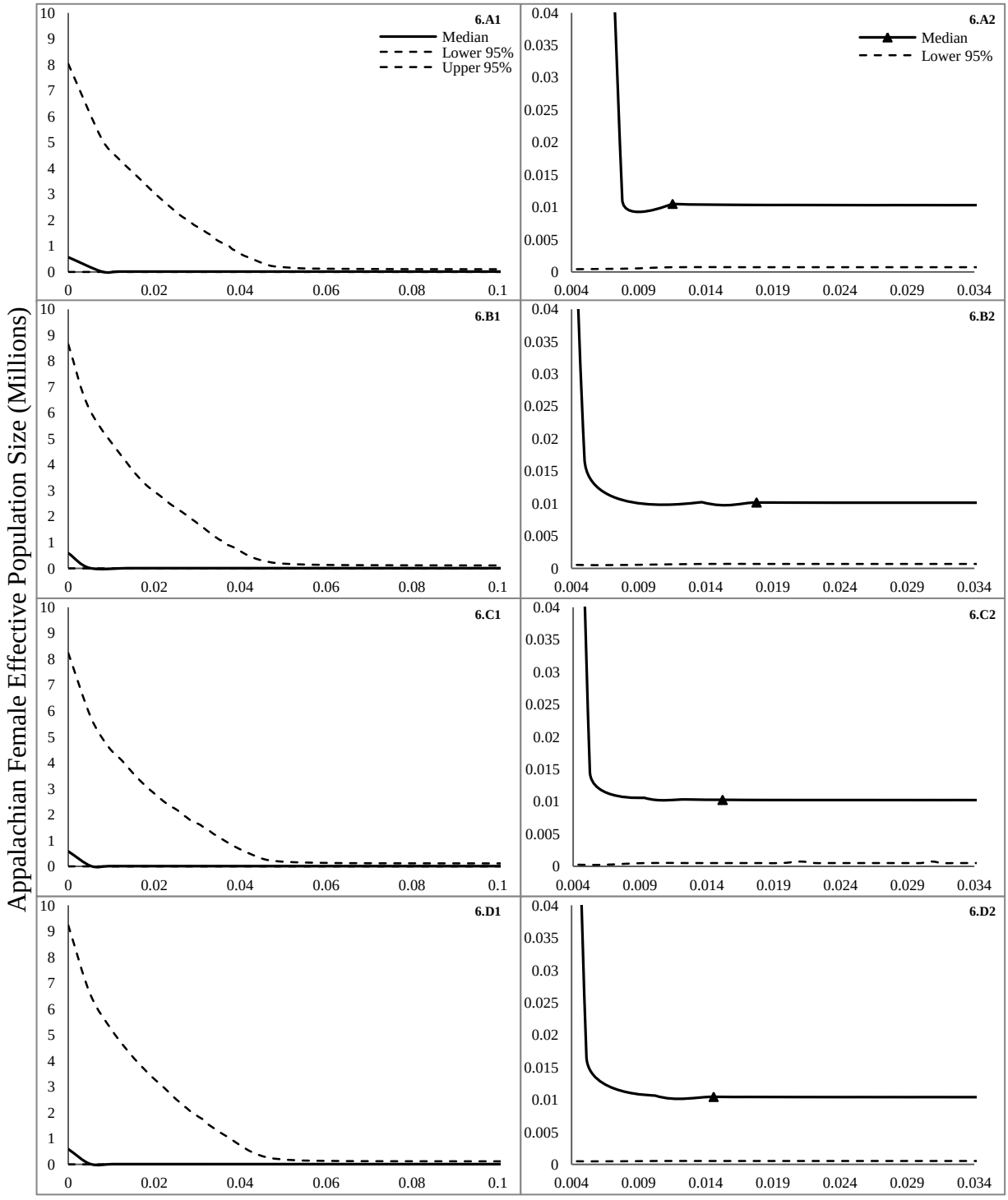

Figure 6. Effective female population size change over time in the Appalachian *P. subflavus* population. Results of four Extended Bayesian Skyline BEAST runs for the Appalachian population support population growth by an order of magnitude. Figures in the first column (5.A1, 5.B1, 5.C1, 5.D1) show the EBSP, and figures in the second column (5.A2, 5.B2, 5.C2, 5.D2) show a magnified view of the EBSP from column 1. The time at which the population change began is marked (▲).

Figure 7

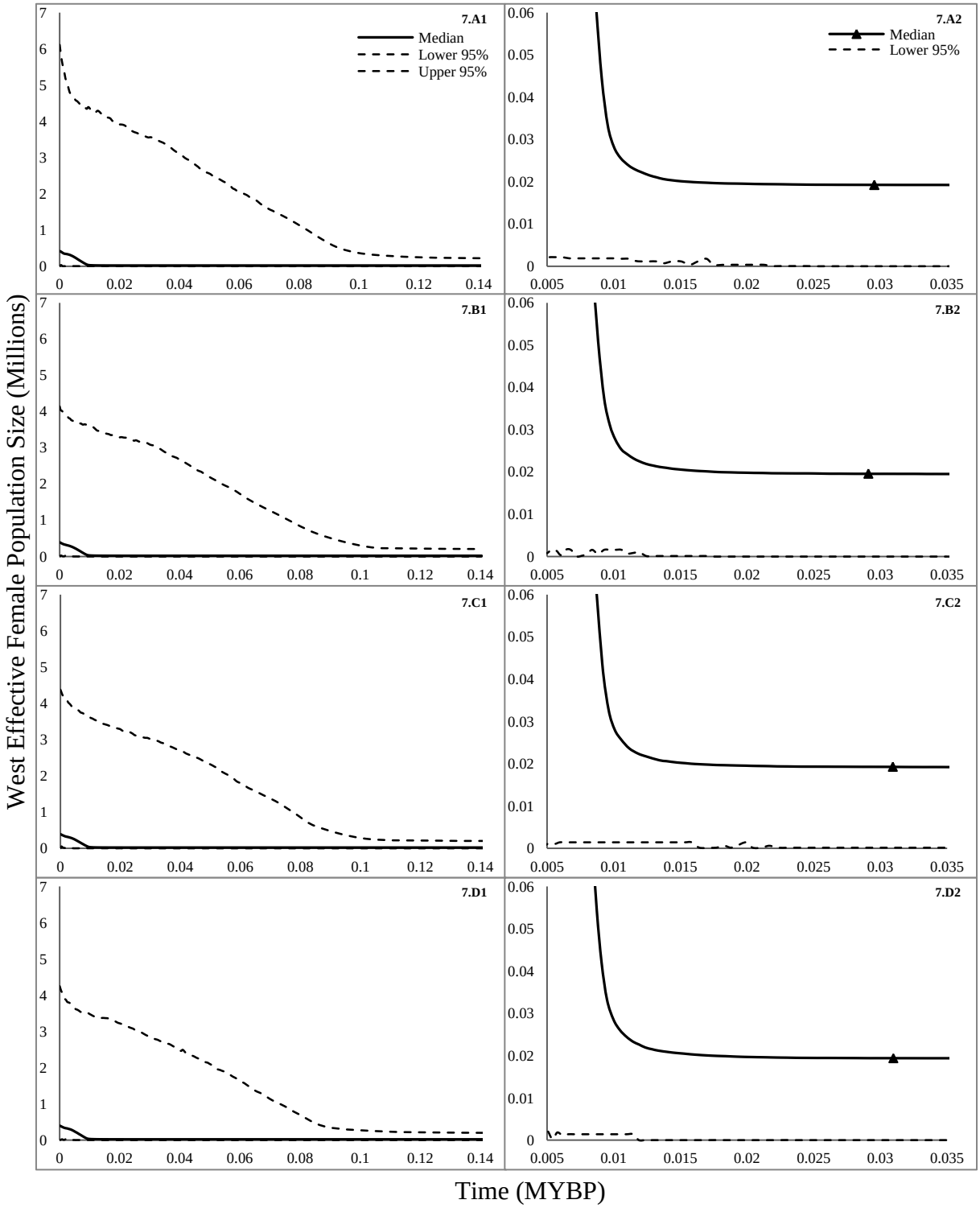

Figure 7. Effective female population size change over time in the West *P. subflavus* population. Four Extended Bayesian Skyline Plots from BEAST show growth in the West population, with the time of growth initiation around thirty thousand years ago. Figures in the first column (6.A1, 6.B1, 6.C1, 6.D1) show the EBSP, and figures in the second column (6.A2, 6.B2, 6.C2, 6.D2) show a magnified view of the EBSP from column 1. The time at which the population change began is marked (▲).

Table 10. The current female effective population size and number of population size changes for two populations of *P. subflavus* over four BEAST analyses. Time of change and ancestral population size were derived from the EBSPs. The values reported for each run are the medians, and the combined values are the means of the medians.

Population	Current Female Effective Population Size (N_0)		Number of Changes in Population Size over Time		Ancestral Female Effective Population Size (N_1)	
Run	Median	95% HPD Interval	Mode	95% HPD Interval	Time of Change (YBP)	Ancestral Size
App. Run 1	$3.73x10^5$	[0.0138 - $7.38x10^6$]	1	[1, 2]	11508.7	$1.05x10^4$
App. Run 2	$4.02x10^5$	[0.0059 - $8.25x10^6$]	1	[1, 2]	17772.4	$1.02x10^4$
App. Run 3	$3.88x10^5$	[0.0103 - $7.53x10^6$]	1	[1, 2]	15182.5	$1.03x10^4$
App. Run 4	$3.97x10^5$	[0.0100 - $8.21x10^6$]	1	[1, 2]	14575.8	$1.04x10^4$
Combined	$3.90x10^5$	[0.0059 - $7.82x10^6$]	1	[1, 2]	14759.9 (±1286.4 S.E.)	$1.03x10^4$ (±76.1 S.E)
West Run 1	$3.34x10^5$	[0.0149 - $5.16x10^6$]	1	[1, 4]	29561.2	$1.92x10^4$
West Run 2	$3.68x10^5$	[0.0188 - $3.83x10^6$]	1	[1, 3]	20897.3	$1.96x10^4$
West Run 3	$3.73x10^5$	[0.0163 - $4.17x10^6$]	1	[1, 3]	30926.2	$1.93x10^4$
West Run 4	$3.83x10^5$	[0.0163 - $4.04x10^6$]	1	[1, 3]	30964.6	$1.93x10^4$
Combined	$3.86x10^5$	[0.0149 - $4.30x10^6$]	1	[1, 3]	28087.3 (±2418.8 S.E.)	$1.94x10^4$ (±77.1 S.E)

Figure 8

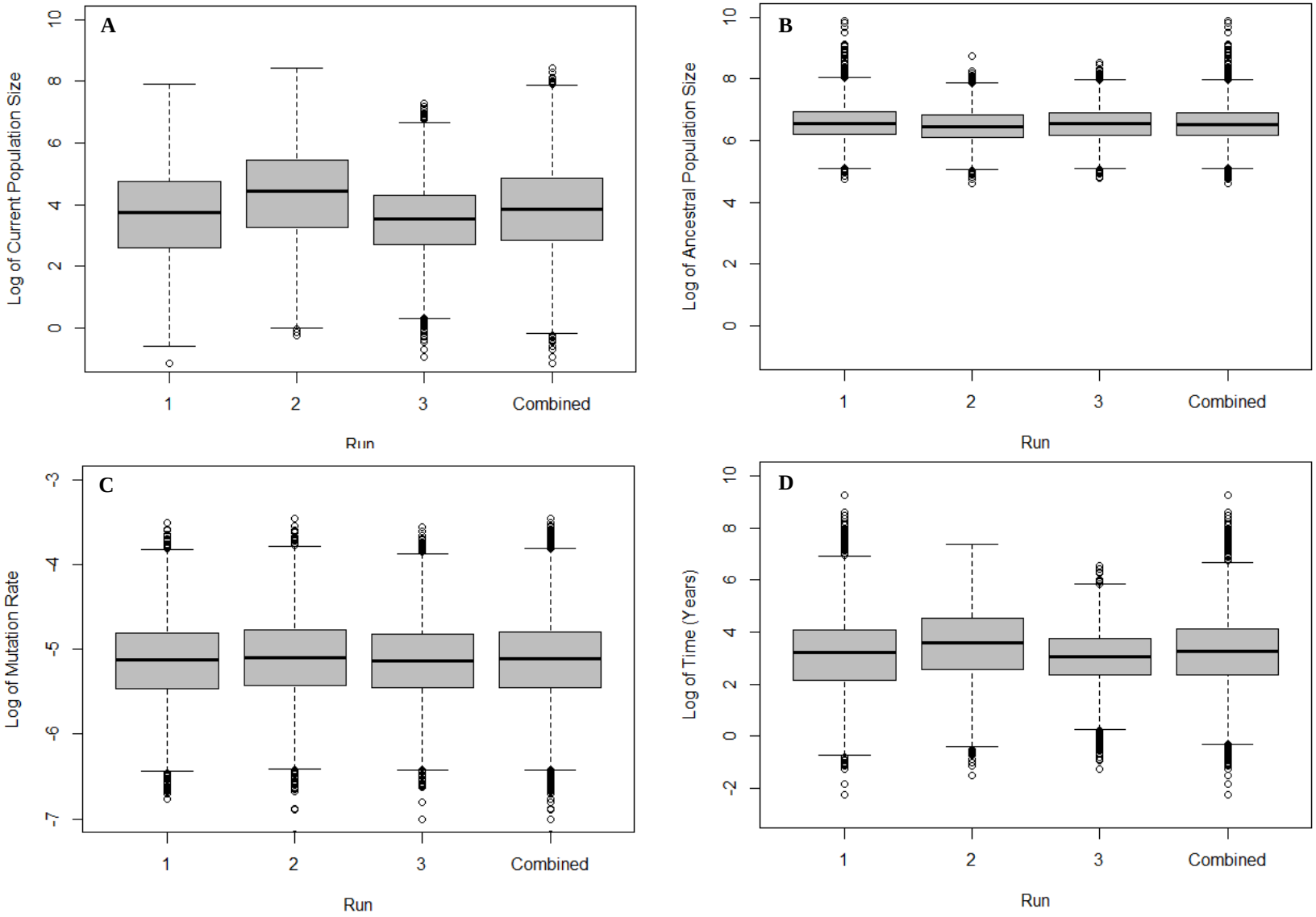
A
Log of Current Population Size
0
2
4
6
8
10
1
2
3
Combined
Run
B
Log of Ancestral Population Size
0
2
4
6
8
10
1
2
3
Combined
Run
C
Log of Mutation Rate
-3
-4
-5
-6
-7
1
2
3
Combined
Run
D
Log of Time (Years)
-2
0
2
4
6
8
10
1
2
3
Combined
Run

Figure 8. The $\log_{10}$ values of N_0, N_1, mu and Ta from three analyses in MSVAR of seven microsatellite loci. A. Estimates of the current effective population size. B. Estimates of the ancestral population size. C. Estimates of the mutation rate, mu, are shown as an average rate across all seven loci. D. The change in size from N_1 to N_0 started at time Ta years in the past. The results of all three runs are combined for each parameter.

Table 11. The mode and 95% HPD for variables N_0, N_1, mu, and Ta from three analyses of MSVAR using seven microsatellite loci. MSVAR output values for current population size (N_0), ancestral population size (N_1), mutation rate (mu), and the time when the population size change from N_1 to N_0 started (Ta). The Ta parameter is presented in units of years. Results from individual analyses are shown (1-3), which utilized independent subsamples of 80 chromosomes. The compilation of results across the three runs is represented by the "Combined" row.

Analysis	Mode N_0	95% HPD N_0	Mode N_1	95% HPD N_1	N_0/ N_1	Mode Ta	95% HPD Ta	Mode Mu	95% HPD Mu
1	759	[.000004 - 1.61×10^6]	3.13×10^6	[0.0301 - 4.55×10^7]	0.443	1922.7	[0.00002 - 4.60×10^5]	9.64×10^{-7}	[0.0801 - 6.56×10^{-5}]
2	15678	[0.00002 - 6.74×10^6]	2.06×10^6	[0.0266 - 2.89×10^7]	0.664	8236.1	[0.00005 - 9.38×10^5]	1.02×10^{-5}	[0.0989 - 8.23×10^{-5}]
3	2668	[0.0002 - 6.78×10^5]	6.51×10^6	[0.0312 - 3.82×10^7]	0.503	20.848	[0.00008 - 1.22×10^5]	7.03×10^{-6}	[0.0873 - 6.59×10^{-5}]
Combined	9262	[0.00001 - 3.78×10^6]	3.13×10^6	[0.0268 - 3.49×10^6]	0.611	1029.7	[0.00003 - 3.85×10^5]	9.64×10^{-7}	[0.0827 - 7.63×10^{-5}]

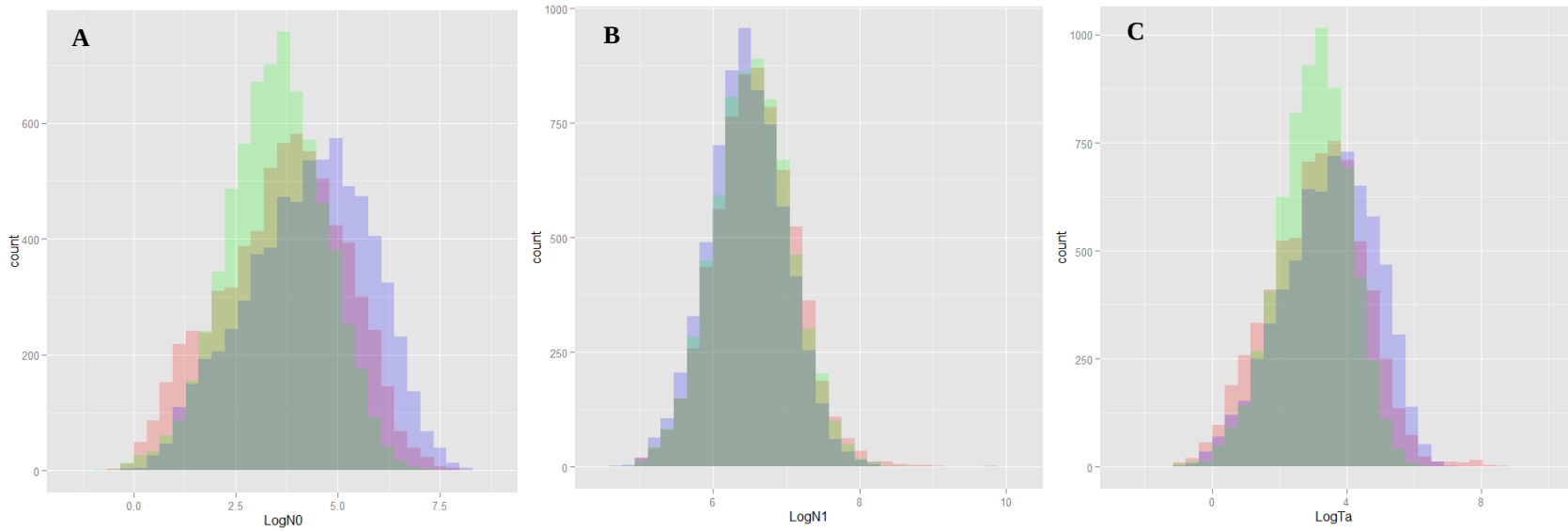

Figure 9. Posterior distributions of log(N_0), log(N_1), and log(Ta) values. The distributions show A. log(N_0), B. log(N_1), and C. log(Ta) values across three separate runs (red, green, and blue). Variation was seen among and within runs, with values of log(N_0) ranging from -1.16 to 8.41, and log(N_1) ranging 4.61 to 9.89. Across the runs, log(Ta) had a range of -2.24 to 9.25.

LITERATURE CITED

Altringham JD. 2011. *Bats from Evolution to Conservation* Second Edition (JD Altringham Ed.). Oxford University Press, Oxford, +284 pp.

Arnett EB, Brown WK, Erickson WP, Fiedler JK, and BL Hamilton. 2010. Patterns of bat fatalities at wind energy facilities in North America. *The Journal of Wildlife Management* 72(1): 61-72.

Arnett EB, and EF Baerwald. 2013. Impacts of wind energy development on bats: implications for conservation. Pp. 435-456, in *Bat Evolution, Ecology, and Conservation* (RA Adams, and SC Pedersen Eds.) Springer Science and Business, New York, + 547 pp.

Arnold BD. 2007. Population structure and sex-biased dispersal in the forest dwelling vespertilionid bat, *Myotis septentrionalis*. *The American Midland Naturalist* 157(2): 374-384.

Barbour RW, and WH Davis. 1969. *Pipistrellus subflavus*. Pp. 115-120, in *Bats of America* (RW Barbour, and WH Davis Eds.). The University Press of Kentucky, Lexington, +286.

Beaumont MA. 1999. Detecting population expansion and decline using microsatellites. *Genetics* 150(4): 2013-2029.

Beaumont MA. 2003. Estimation of population growth or decline in genetically monitored populations. *Genetics* 164(3): 1139-1160.

Bellemain E, Swenson JE, Tallmon D, Brunberg S, and P Taberlet. 2005. Estimating population size of elusive animals with DNA from hunter-collected feces: four methods for brown bears. *Conservation Biology* 19(1): 150-161.

Bermingham E, and C Moritz. 1998. Comparative phylogeography: concepts and applications. *Molecular Ecology* 7:367-369.

Boyles JG, Cryan PM, McCracken GF, and TH Kunz. 2011. Economic importance of bats in agriculture. *Science* 332(6025): 41-42.

Buchalski MR, Chaverri G, and MJ Vonhof. 2014. When genes move farther than offspring: gene flow by male gamete dispersal in the highly philopatric bat species *Thyroptera tricolor*. *Molecular Ecology* 23(2): 464-480.

Burland TM, and J Worthington Wilmer. 2001. Seeing in the dark: molecular approaches to the study of bat populations. *Biological Reviews* 76: 389-409.

Carstens BC, Sullivan J, Dávalos LM, Larsen PA, and SC Pedersen. 2004. Exploring population genetic structure in three species of Lesser Antillean bats. *Molecular Ecology* 13(9): 2557-2566.

Castella V, and M Ruedi. 2000. Characterization of highly variable microsatellite loci in the bat *Myotis myotis* (Chiroptera: Vespertilionidae). *Molecular Ecology* 9: 1000-1002.

Chen SF, Rossiter SJ, Faulkes CG, and G Jones. 2006. Population genetic structure and demographic history of the endemic Formosan lesser horseshoe bat (*Rhinolophus monoceros*). *Molecular Ecology* 15: 1643-1656.

Chen SF, Jones G, and SJ Rossiter. 2008. Sex-biased gene flow and colonization in the Formosan lesser horseshoe bat: inference from nuclear and mitochondrial markers. *Journal of Zoology* 274(3): 207-215.

Cryan PM, and JP Veilleux. 2007. Migration and use of autumn winter and spring roosts by tree bats. Pp. 153-175, in *Bats in Forests: Conservation and Management* (Lacki MJ, Hayes JP, and A Kurta Eds.) Johns Hopkins University Press, Baltimore, +352 pp.

Cryan PM, and RM Barclay. 2009. Causes of bat fatalities at wind turbines: hypotheses and predictions. *Journal of Mammalogy* 90(6): 1330-1340.

Cryan PM, Meteyer CU, Boyles JG, and DS Blehert. 2010. Wing pathology of white-nose syndrome in bats suggests life-threatening disruption of physiology. *BMC Biology* 8**:** e135.

Darriba D, Toboada GL, Doallo R, and D Posada. 2012. jModelTest 2: more models, new heuristics and parallel computing. *Nature Methods* 9(8): 772.

Daszak P, Cunningham AA, and AD Hyatt. 2001. Anthropogenic environmental change and the emergence of infectious disease in wildlife. *Acta Tropica* 78(2): 103-116.

Drummond AJ, Rambaut A, Shapiro B, and OG Pybus. 2005. Bayesian coalescent inference of past population dynamics from molecular sequences. *Molecular Biology and Evolution* 22(5): 1185-1192.

Drummond AJ, and A Rambaut. 2007. BEAST: Bayesian evolutionary analysis by sampling trees. *BMC Evolutionary Biology* 7: e214.

Drummond AJ, Suchard MA, Xie D, and A Rambaut. 2012. Bayesian phylogenetics with BEAUti and the BEAST 1.7. *Molecular Biology and Evolution* 29(8): 1969-1973.

Duchesne P, and J Turgeon. 2012. FLOCK provides reliable solutions to the "number of populations" problem. *Journal of Heredity* 103(5): 734-743.

Duchesne P, Méthot J, and J Turgeon. 2013. FLOCK 3.1 User Guide. Département de biologie, Université Laval. http://www.bio.ulaval.ca/no_cache/en/department/professors/professors/professeur/11/13/.

Eggert LS, Eggert JA, and DS Woodruff. 2003. Estimating population sizes for elusive animals: the forest elephants of Kakum National Park, Ghana. *Molecular Ecology* 12(6): 1389-1402.

Escorza-Treviño S, and AE Dizon. 2000. Phylogeography, intraspecific structure and sex-biased dispersal of Dall's porpoise, *Phocoenoides dalli,* revealed by mitochondrial and microsatellite DNA analyses. *Molecular Ecology* 9(8): 1049-1060.

Evanno G, Regnaut S, and J Goudet. 2005. Determining the number of clusters of individuals using the software STRUCTURE: a simulation study. *Molecular Ecology* 14:2611-2620.

Excoffier L, Guillaume L, and S Schneider. 2007. Arlequin (version 3.0): an integrated software package for population genetics data analysis. *Evolutionary Bioinformatics* 1: 47-50.

Farrow LJ, and HG Broders. 2011. Loss of forest cover impacts the distribution of the forest-dwelling tri-colored bat (*Perimyotis subflavus*). *Mammalian Biology* 76: 172-179.

Fisher RA. 1930. *The Genetical Theory of Natural Selection*. Oxford University Press, Oxford.

Fleming TH, and P Eby. 2003. Ecology of bat migration. Pp. 156-208, in *Bat Ecology* (TH Kunz, and MB Fenton Eds.) University of Chicago Press, Chicago, +743 pp.

Frankham R. 1995. Effective population size/adult population size ratios in wildlife: a review. *Genetical Research* 66: 95-107.

Fraser EE, McGuire LP, Eger JL, Longstaffe FJ, and MB Fenton. 2012. Evidence of latitudinal migration in *Perimyotis subflavus*. *PLoS ONE* 7(2): e0031419.

Fuentes-Montemayor E, Goulson D, Cavin L, Wallace JM, and KJ Park. 2013. Fragmented woodlands in agricultural landscapes: the influence of woodland character and landscape context on bats and insect prey. *Agriculture, Ecosystems and Environment* 172: 6-15.

Fujita MS, and TH Kunz. 1984. *Pipistrellus subflavus*. *Mammalian Species* 228: 1-6.

Furmankiewicz J, and J Altringham. 2007. Genetic structure in a swarming brown long-eared bat (*Plecotus auritus*) population: evidence for mating at swarming sites. *Conservation Genetics* 8(4): 913-923.

Galtier N, Nabholz B, Glemin S, and GDD Hurst. 2009. Mitochondrial DNA as a marker of molecular diversity: reappraisal. *Molecular Ecology* 18(22): 4541-4550.

Gayevskiy V, Klaere S, Knight S, and MR Goddard. 2014. ObStruct: a method to objectively analyse factors driving population structure using Bayesian ancestry profiles. *PLoS ONE* 9(1): e85196.

Gelman A, and DB Rubin. 1992. Inference from iterative simulation using multiple sequences. *Statistical Science* 7: 457–511.

Greenwood PJ. 1980. Mating systems, philopatry and dispersal in birds and mammals. *Animal Behavior* 28: 1140-1162.

Griffin DR. 1940. Migrations of New England bats. *Bulletin of the Museum of Comparative Zoology* 86: 217-246.

Guschanski K, Vigilant L, McNeilage A, Gray M, Kagoda E, and MM Robbins. 2009. Counting elusive animals: comparing field and genetic census of the entire mountain gorilla population of Bwindi Impenetrable National Park, Uganda. *Biological Conservation* 142(2): 290-300.

Handley LJL, and N Perrin. 2007. Advances in our understanding of mammalian sex-biased dispersal. *Molecular Ecology* 16: 1559-1578.

Hare MP, Nunney L, Schwartz MK, Ruzzante DE, Burford M, Waples RS, Ruegg K, and F Palstra. 2011. Understanding and estimating effective population size for practical application in marine species management. *Conservation Biology* 25(3): 438-449.

Heled J, and AJ Drummond. 2008. Bayesian inference of population size history from multiple loci. *BMC Evolutionary Biology* 8: e289.

Heled J. 2010. Extended Bayesian skyline plot tutorial. 20 April 2014. http://www.beast-mcmc.googlecode.com.

Heller R, Okello JBA, and H Siegismund. 2010. Can small wildlife conservancies maintain genetically stable populations of large mammals? Evidence for increased genetic drift in geographically restricted populations of Cape buffalo in East Africa. *Molecular Ecology* 19: 1324-1334.

Ho SYW, and B Shapiro. 2011. Skyline-plot methods for estimating demographic history from nucleotide sequences. *Molecular Ecology* 11:423-434.

Kerth G, Mayer F, and E Petit. 2002. Extreme sex-biased dispersal in the communally breeding, nonmigratory Bechstein's bat (*Myotis bechsteinii*). *Molecular Ecology* 11(8): 1491-1498.

Kerth G, Kiefer A, Trappman C, and M Weishaar. 2003. High gene diversity at swarming sites suggest hot spots for gene flow in endangered Bechstein's bat. *Conservation Genetics* 4(4): 491-499.

Kimura M. 1981. Estimation of evolutionary distances between homologous nucleotide sequences. *Proceedings of the National Academy of Sciences, USA* 78:454-458.

Kingman JFC. 1982. The coalescent. *Stochastic Processes and their Applications* 13: 235-238.

Krauel JJ, and GF McCracken. 2013. Recent advances in bat migration. Pp 293-307, in *Bat Evolution, Ecology, and Conservation* (RA Adams, and SC Pederson Eds.) Springer Science and Business, New York, +531 pp.

Kunz TH, Betke M, Hristov NI, and MJ Vonhof. 2009. Methods for assessing colony size, population size, and relative abundance of bats. Pp. 133-157, in *Ecological and Behavioral Methods for the Study of Bats,* 2nd Edition (Kunz TH, and S Parsons Eds.) Johns Hopkins University Press, Baltimore, +901 pp.

Kurta A. 2010. Reproductive timing, distribution, and sex ratios of tree bats in lower Michigan. *Journal of Mammalogy* 91(3): 586-592.

Lee DN, Howell JM, and RA Van Den Bussche. 2011. Development and characterization of 15 polymorphic tetranucleotide microsatellite loci for Townsend's big-eared bat (*Corynorhinus townsendii*) and cross amplification in Rafinesque's big-eared bat (*Corynorhinus rafinesquii*). *Conservation Genetics Resources* 4(2): 429-433.

Lu G, Lin A, Lou J, Blondel DV, Meiklejohn KA, Sun K, and J Feng. 2013. Phylogeography of the Rickett's big-footed bat, *Myotis pilosus* (Chiroptera: Vespertilionidae): a novel pattern of genetic structure of bats in China. *BMC Evolutionary Biology* 13: e241.

Luikart G, Sherwin WB, Steele BM, and FW Allendorf. 1998. Usefulness of molecular markers for detecting population bottlenecks via monitoring genetic change. *Molecular Ecology* 7(8): 963-974.

Luikart G, Ryman N, Tallmon DA, Schwartz MK, and FW Allendorf. 2010. Estimation of census and effective population sizes: the increasing usefulness of DNA-based approaches. *Conservation Genetics* 11: 355-373.

McCracken GF, and GS Wilkinson. 2000. Bat mating systems. Pp. 321-362, in *Reproductive Biology of Bats* (EG Crichton, and PH Krutzsch Eds.) Academic Press, New York, +510pp.

Meirmans PG. 2006. Using the AMOVA framework to estimate a standardized genetic differentiation measure. *Evolution* 60: 2399-2402.

Miller-Butterworth CM, Vonhof MJ, Rosenstern J, Turner GC, and AL Russell. 2014. Genetic structure of little brown bats (*Myotis lucifigus*) corresponds with spread of white-nose syndrome among hibernacula. *Journal of Heredity* 105(3): 354-364.

Moussy C, Hosken DJ, Mathews F, Smith GC, Aegerter JN, and S Bearhop. 2013. Migration and dispersal patterns of bats and their influence on genetic structure. *Mammal Review* 43: 183-195.

Nagy M, Günther L, Knŏrnschild M, and F Mayer. 2013. Female-biased dispersal in a bat with a female-defence mating strategy. *Molecular Ecology* 22(6): 1733-1745.

O'Connor KE, Herzog CJ, Hicks AC, and RI von Linden. 2011. Looking at population declines of cave bats through summer mist netting. Oral presentation at 2nd Joint Meeting of the Northeastern Bat Working Group, Midwest Bat Working Group, and Southeastern Bat Diversity Network. Louisville, KY.

O'Corry-Crowe GM, Suydam RS, Rosenberg A, Frost KJ, and AE Dizon. 1997. Phylogeography, population structure and dispersal patterns of the beluga whale *Delphinapterus leucas* in the western Nearctic revealed by mitochondrial DNA. *Molecular Ecology* 6(10): 955-970.

Oyler-McCance S, and J Fike. 2011. Characterization of small microsatellite loci isolated in endangered Indiana bat (*Myotis sodalis*) for use in non-invasive sampling. *Conservation Genetics Resources* 3(2): 243-245.

Parsons KN, Jones G, and F Greenway. 2003. Swarming activity of temperate zone microchiropteran bats: effects of season, time of night and weather conditions. *Journal of Zoology* 261(3): 257-264.

Peakall R, and PE Smouse. 2012. GenAlEx 6.5: genetic analysis in Excel, population genetic software for teaching and research-an update. *Bioinformatics* 28: 2537-2539.

Petit E, Balloux F, and J Goudet. 2001. Sex-biased dispersal in a migratory bat: a characterization using sex-specific demographic parameters. *Evolution* 55(3): 635-640.

Piaggio AJ, Navo KW, and CW Stihler. 2009a. Intraspecific comparison of population structure, genetic diversity, and dispersal among three subspecies of Townsend's big-eared bats, *Corynorhinus townsendii townsendii*, *C. t. pallescens*, and the endangered *C. t. virginianus*. *Conservation Genetics* 10(1): 143-159.

Piaggio AJ, Figueroa JA, and SL Perkins. 2009b. Development and characterization of 15 polymorphic microsatellite loci isolated from Rafinesque's big-eared bat, *Corynorhinus rafinesquii*. *Molecular Ecology Resources* 9: 1191-1193.

Pimm SL, Russell GJ, Gittleman JL, and TM Brooks. 1995. The future of biodiversity. *Science* 269: 347-350.

Pimm SL, Jenkins CN, Abell R, Brooks TM, Gittleman JL, Joppa LN, Raven PH, Roberts CM, and JO Sexton. 2014. The biodiversity of species and their rates of extinction, distribution, and protection. *Science* 344: 987.

Poisssant JA. 2009. Roosting and social ecology of the tricolored bat, *Perimyotis subflavus*, in Nova Scotia. Master of Science Thesis. Saint Mary's University: Halifax, Nova Scotia.

Posada D. 2008. jModelTest: Phylogenetic model averaging. *Molecular Biology and Evolution* 25: 1253-1256.

Pritchard JK, Stephens M, and P. Donnelly. 2000. Inference of population structure using multilocus genotype data. *Genetics* 155: 945-959.

Prugnolle F, and T de Meeus. 2002. Inferring sex-biased dispersal from population genetic tools: a review. *Heredity* 88: 161-165.

Pybus OG, Rambaut A, and PH Harvey. 2000. An integrated framework for the inference of viral population history from reconstructed genealogies. *Genetics* 155: 1429-1437.

R Development Core Team. 2008. R: A language and environment for statistical computing. R Foundation for Statistical Computing, Vienna, Austria. http://www.R-project.org.

Reeder DM, and MS Moore. 2013. White-nose syndrome: a deadly emerging infectious disease of hibernating bats. Pp. 413-434, in *Bat Evolution, Ecology, and Conservation* (RA Adams, and SC Pedersen Eds.) Springer Science and Business, New York, + 547 pp.

Rivers NM, Butlin RK, and JD Altringham. 2005. Genetic population structure of Natterer's bats explained by mating at swarming sites and philopatry. *Molecular Ecology* 14(14): 4299-4312.

Rivers NM, Butlin RK, and JD Altringham. 2006. Autumn swarming behaviour of Natter's bats in the UK: population size, catchment area and dispersal. *Biological Conservation* 127(2): 215-226.

Rocha LA, Craig MT, and BW Bowen. 2007. Phylogeography and the conservation of coral reef fishes. *Coral Reefs* 26(3): 501-512.

Rousset F. 1997. Genetic differentiation and estimation of gene flow from *F*-statistics under isolation by distance. *Genetics* 145: 1219-1228.

Russell AL, Medellín RA, and GF McCracken. 2005. Genetic variation and migration in the Mexican free-tailed bat (*Tadarida brasiliensis mexicana*). *Molecular Ecology* 14(7): 2207-2222.

Safi K, Konig B, and G Kerth. 2007. Sex differences in population genetics, home range size and habitat use of the parti-colored bat (*Vespertilio murinus*, Linnaeus 1758) in Switzerland and their consequences for conservation. *Biological Conservation* 137: 28-36.

Santana QC, Coetzee MPA, Steenkamp ET, Mlonyeni OX, Hammond GNA, Wingfield MJ, and BD Wingfield. 2009. Microsatellite discovery by deep sequencing of enriched genomic libraries. *BioTechniques* 46: 217-223.

Segelbacher G, Cushman SA, Epperson BK, Fortin MJ, Fracois O, Hardy OJ, Holderegger R, Taberlet P, Watis LP, and S Manel. 2009. Applications of landscape genetics in conservation biology: concepts and challenges. *Conservation Genetics* 11(2): 375-385.

Senior P, Butlin RK, and JD Altringham. 2005. Sex and segregation in temperate bats. *Proceedings of the Royal Society B: Biological Sciences* 272: 2467-3473.

Slatkin M. 1995. A measure of population subdivision based on microsatellite allele frequencies. *Genetics* 139(1): 457-462.

Smith KF, Acevedo-Whitehouse K, and AB Pedersen. 2009. The role of infectious diseases in biological conservation. *Animal Conservation* 12: 1–12.

Storz JF, and MA Beaumont. 2002. Testing for genetic evidence of population expansion and contraction: an empirical analysis of microsatellite variation using a hierarchical Bayesian model. *Evolution* 56(1): 154-166.

Sun YH, Monagin C, Liu XS, and JP Chen. 2012. A test for sex-biased dispersal in *Cynopterus spinx*: inferences from microsatellite markers and mitochondrial DNA. *Acta Chiropterologica* 14(1): 39-44.

Tautz D. 1989. Hypervariability of simple sequences as a general source for polymorphic markers. *Nucleic Acids Research* 17: 6463-6471.

Trujillo RG, and SK Amelon. 2009. Development of microsatellite markers in *Myotis sodalis* and cross-species amplification in *M. gricescens, M. leibii, M. lucifugus*, and *M. septentrionalis*. *Conservation Genetics* 10: 1965-1968.

Turmelle AS, Kunz TH, and MD Sorenson. 2011. A tale of two genomes: contrasting patterns of phylogeographic structure on a widely distributed bat. *Molecular Ecology* 20(2): 357-375.

Veilleux JP, and SL Veilleux. 2004. Intra-annual and interannual fidelity to summer roost areas by female eastern pipistrelles, *Pipistrellus subflavus*. *American Midland Naturalist* 152(1): 196-200.

Vignal A, Milan D, SanCristobal M, and A Eggen. 2002. A review on SNP and other types of molecular markers and their use in animal genetics. *Genetics Selection Evolution* 34: 275-305.

Vonhof MJ, Strobeck C, and MB Fenton. 2008. Genetic variation and population structure in big brown bats (*Eptesicus fuscus*): is female dispersal important? *Journal of Mammalogy* 89(6): 1411-1419.

Vonhof MJ, and AL Russell. 2013. Genetic approaches to understanding the population-level impact of wind energy development on migratory bats. Technical Report, U.S. Department of Energy.

Wilkinson GS, and AM Chapman. 1991. Length and sequence variation in evening bat d-loop mtDNA. *Genetics* 128: 607-617.

Williams ES, Yuill T, Artois M, Fischer J, and SA Haigh. 2002. Emerging infectious diseases in wildlife. *Revue scientifique et technique (International Office of Epizootics)* 21(1): 139-157.

Worthington Wilmer J, and E Barratt. 1996. A non-lethal method of tissue sampling for genetic studies of chiropterans. *Bat Research News* 37: 1-3.

Wright S. 1931. Evolution in Mendelian populations. *Genetics* 16: 97-159.

Xu L, He C, Shen C, Jiang T, Shi L, Sun K, Berquist SW, and J Feng. 2010. Phylogeography and population genetic structure of the great leaf-nosed bat (*Hipposideros armiger*) in China. *Journal of Heredity* 101(5): 562-572.